Join MSC-E/MSC-W Report

EMEP/MSC-E Technical Report 1/2012

June 2012

Global scale modelling within EMEP: Progress report

J. E. Jonson and O. Travnikov (Eds.)

Contributing authors:

Alexey Gusev, Nadezhda Batrakova, Olga Rozovskaya, Michael Schulz, Victor Shatalov, Valeriy Sokovykh, Semeena Valiyaveetil

msc-e

Meteorological Synthesizing Centre - East
Krasina pereulok, 16/1
123056 Moscow
Russia
Tel.: +7 495 981 15 67
Fax: +7 495 981 15 66
E-mail: msce@msceast.org
Internet: www.msceast.org

msc-w

Norwegian Meteorological Institute (met.no)
Postboks 43 Blindren
N-01313 Oslo
Norway

Phone: +47 22 96 30 00
Fax: +47 22 96 30 50
E-mail: emep.mscw@met.no
Internet: www.emep.int

Executive Summary

This report was prepared for the 36th session of the Steering body to EMEP. It presents the progress in the development of global modelling at the two EMEP centres MSC-E and MSC-W, as well as other modelling activities related to global scale modelling.

Both centres are contributing to the Task Force on Hemispheric Transport of Air Pollution (TF-HTAP). This task force now has a new workplan running until 2015. Both centres expect to benefit from the co-operation and exchange of information and expertise resulting from the participation to the TF-HTAP. This provides a common platform for further cooperation between the two centres. Furthermore the task force provides opportunities for model inter-comparisons with other global and regional models.

For both centres this report focus on nesting of global to regional model calculations. Due to computational constraints, global models can only be run on a relatively coarse model resolution. However, global model calculations are needed in order to calculate the transcontinental effects pollution. Nesting from global models to regional models that can be run on a finer model resolution, makes it possible to study the regional/local effects of trans-continental pollution on a much finer scale than with global model calculations alone. At MSC-W the focus in these calculations is on tropospheric ozone, whereas MSC-E focus on mercury. For surface ozone lateral boundary concentrations are shown to have marked effects. Concentrations of Hg0 in Europe are dominated by the amount of Hg0 transported via the boundaries into the model domain.

At both centers the effects of the temporal resolution of the lateral boundary concentrations are tested. The results indicate that the difference between simulation with 6-hour, daily and monthly BCs is insignificant over the main part of continental Europe but can be noticeable only over the periphery areas. For the calculation of short term episodes frequent updates (every 6 hours) may however be needed.

At MSC-E the GLEMOS model has been used to calculate the historical accumulation of hexachlorobenzene (HCB) on a global scale. The calculations show that the spatial pattern of HCB in the atmosphere is mainly determined by the re-emissions of historically accumulated HCB from the ground.

This report also includes a literature study of the cycling of mercury in seawater with the aim of improving the description of the multi-media processes in future versions of the models at MSC-E.

CONTENTS

Introduction

There is an increasing awareness that air pollutants can be transported between continents. The relative contribution from intercontinental sources, and the frequency of such pollution events, will wary by species, time of year and source type (TF-HTAP, 2010). For advection from other distant continents to be of any significance the lifetime of the pollutant(s) (and/or their precursors) in the atmosphere has to be of the same magnitude or longer than the advection time. In order to include the contributions from distant sources the model domain should be global (or at least hemispheric), and this restricts the refinement of the grid resolution that can be used in these calculations. Very few, if any global chemical tracer models have a horizontal grid resolution better than 1 x 1 degree. At 60 degrees north this corresponds to an approximate 56 km x 112 km resolution. Regional model calculations can be made on a much finer grid resolution. With the EMEP model regional calculations for Europe have traditionally been made on an approximate 50 x 50 km^2 resolution, but calculations are frequently made on finer grid scales.

Many of the air pollutants of concern have typical residence times in the atmosphere ranging from several days to months. Previous studies (HTAP, 2010) have shown that ozone, some POPs and mercury in particular have relatively long lifetimes in the troposphere, and that there is a substantial intercontinental contribution. For PM, with typical lifetimes of a few days only, the intercontinental contributions are small in general, but with significant episodic contributions.

As a result of a continuous process of model development the reliability of the predictions from both global and regional models are improving. In order to increase our confidence in the chemical and physical processes in specific regions, regional model runs are made on fine scale resolutions that as yet can not be achieved by global models due to CPU limitations. In most cases the regional models then use a simplified set of boundary concentrations. As a result the transient nature of the influx across the lateral boundaries is not fully accounted for. Furthermore, with this approach the origin of the pollutants can not be attributed to any particular source type and/or region.

For both the EMEP photochemistry model at MSC-W and the GLEMOS model at MSC-E, regional model calculations are nested into the global model results. In the regional scale calculations concentrations from the global model are provided at the lateral boundaries as a curtain. Several sensitivity test are made varying the frequency of when the lateral boundaries are updated. In adition, different lengths of the regional model sipin-up were evaluated as well as sensitivity of the model results to sets of boundary conditions generated by different global models.

In particular, it was obtained with the GLEMOS model that air concentrations of mercury in Europe are dominated by boundary conditions (mostly Hg^0), whereas local emissions of the oxidised forms (Hg^{2+} and PHg) may be important for regional deposition. Different temporal resolution of boundary conditions does not significantly affect monthly mean simulation results, but consistency between process parameterisations applied in a regional model and those in a global model generating BCs is critical for regional scale simulations of mercury.

The multi-media GLEMOS model was also applied for the first time for simulation of hexachlorobenzene (HCB) on a global scale. It was shown that spatial pattern of HCB atmospheric concentrations is determined mainly by secondary emission sources, that is, by re-emission from HCB historically accumulated in the underlying surface. Hence, for simulations of HCB contamination levels both in the EMEP region and over the entire globe consideration of historical HCB accumulation is of particular importance.

Development of the multi-media aspect of the GLEMOS model was continued with elaboration of the ocean module for mercury. For this purpose a comprehensive literature survey has been perform to collect available information on mercury cycling in seawater including identification of the key processes and reaction rate constants. The compiled information will be used for elaboration of the mercury chemical scheme in seawater, which will be incorporated to the next version of the model.

1. Global and nested regional calculations: Comparing model results for Europe

Jan Eiof Jonson, Semeena Valiyaveetil and Michael Schulz

As demonstrated in the HTAP (2010) report, the spread in model results between different global models is large, and the subsequent ability to reproduce the measurements somewhat limited. Traditionally, model results from regional models compare better with measurements. At least two factors may help to explain the better performance of regional models versus global models.

1. The chemistry in the atmosphere is nonlinear. A more detailed representation of sources and sinks should increase the model performance, and also improve the representability of the model calculations when compared to measurements at specific locations.

2. The residence times for air in regional models is of the order of days only, comparable to, or shorter than, the lifetime of many air pollutants and/or their precursors. As a result baseline levels of several air pollutants are to a large extent controlled by the boundary concentrations. Such boundary concentrations are often selected based on measurements/climatology, or global model results that are known to give reasonable result in the regional model calculations. In global model calculations inconsistencies in the model input data and/or model parameterizations may build up, resulting in unrealistic concentration levels.

The EMEP model is highly flexible, and can be used on for a wide range of applications. Model resolution and model domain can be easily changed from global to regional with horizontal resolutions ranging from 1 x 1 degrees on a global domain to a few kilometres on regional domains. In this study we compare the model results from global and regional model calculations. Global model calculations have been made on a 1 x 1 degrees resolution, whereas the regional model calculations are made on a 0.2 x 0.2 degrees resolution. For the regional model calculations the following sensitivity tests are made:

1. Regional model calculations with lateral boundary concentrations from the global model calculation read in as 6 hour averages

2. Regional model calculations with lateral boundary concentrations from the global model calculation read in as monthly averages

3. Regional model calculations with lateral boundary concentrations based on a combination of measurements/climatology and model calculations. (see Simpson et al., 2012).

With these sensitivity tests we will test if the model results change/improve as we go down in scale, and to what extent the regional model calculations are affected by the lateral boundary concentrations. Furthermore we will test if there are specific regions that are more affected by scale or choice of lateral boundary concentrations and to what extent there are differences between rural background sites and sites influenced by local/regional sources.

It is important that the model setup for the two model runs are identical in the sense that the only difference is related to scale and model resolution. This requires that we use the same model version and that the model input data (including emissions) are the same where the two model domains overlap.

Over the regional model domain, and the part of the global domain overlapped by the regional domain, the emissions are based on the EMEP emissions for 2008, regridded to the appropriate regional and global model resolution. In the remaining part of the global model domain the emissions have been described in Travnikov et al. (2009).

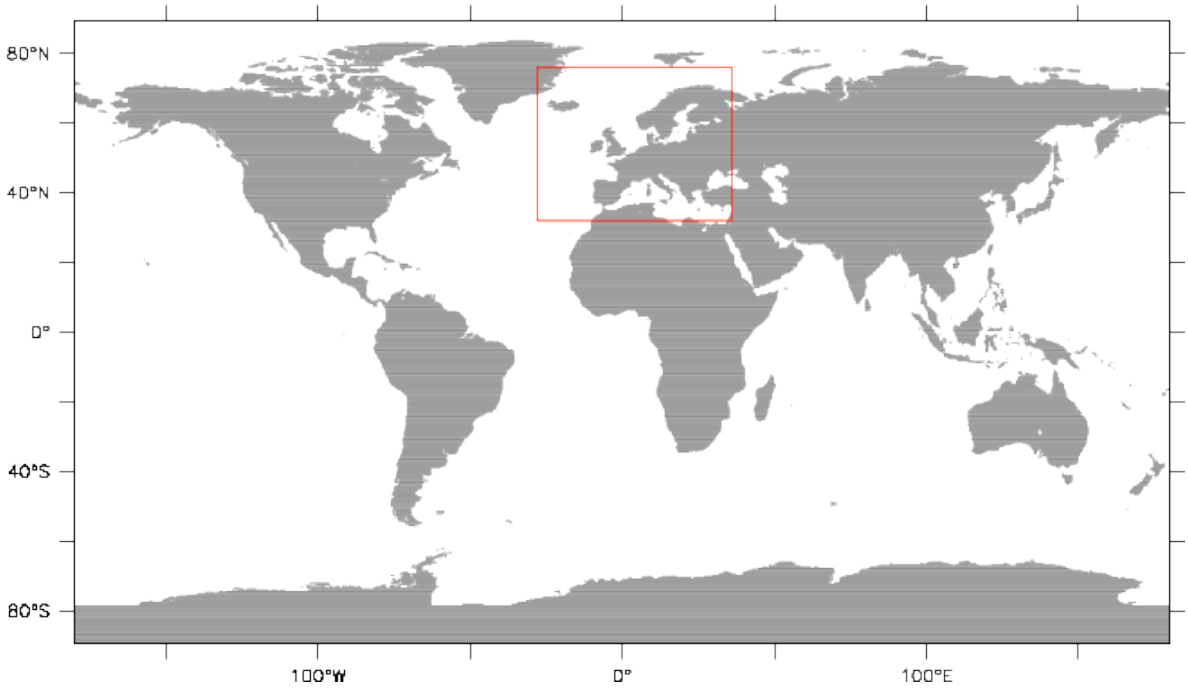

Fig. 1.1 Configuration of the global and regional domains. Global domain with 1 x 1 degrees resolution. Regional, 0.2 x 0.2 degrees domain from 28 degrees west to 36 degrees east and from 32 to 76 degrees north.

1.1 Global and regional nested model result

The main species of interest in this study is ozone, as this species has a lifetime in the atmosphere long enough to be transported between continents. Below we show the global model results and the results from the regional model sensitivity tests, with the main focus on ozone. The model results for the 4 model runs (one global and three regional) have been uploaded to the EAROCOM tool (see www.aerocom.met.no) for validation against the EMEP measurements for 2008 (www.nilu.no/projects/ccc/network/index.html).

Figure 1.1a shows the scatter plot for the regional calculation of ozone with 6 hourly updated BCs against measurements. Figure 1.1b shows the model versus observation bias for the model calculations with 6 hourly updated BCs. The global model calculation and the regional calculation with monthly updated BCs give virtually identical results. Regional calculations using the Mace Head correction as BCs give a slightly lower bias (figures not shown).

.

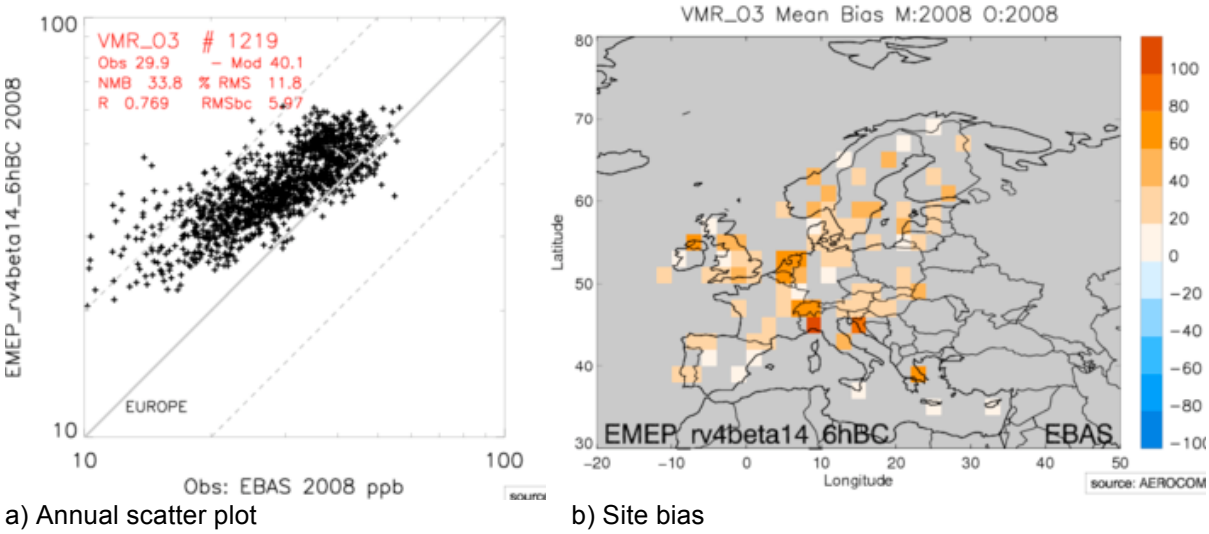

a) Annual scatter plot b) Site bias

Figure 1.1. *Calculated versus observed annual ozone from EMEP (EBAS). a) Scatter plot. b) site bias plot.*

The same results are illustrated by frequency plots or annual daily maximum ozone in Figure 1.2. Compared to measurements, the frequency of the calculated ozone levels is displaced towards higher values, and somewhat more so for the regional model with 6 hourly BSs from the global model. Again results for the global model calculation and the Regional calculations with monthly updated BCs are not shown as these results are virtually identical.

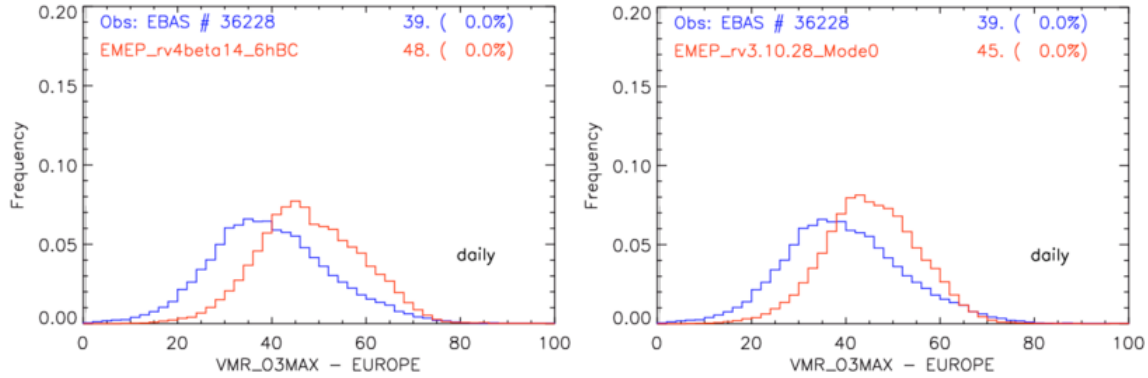

a) Regional calculation with 6h BCs b) Regional calculations with Mace Head

Figure 1.2. *Frequency of measured and model calculated daily maximum ozone in ppb over the full year.*

Figure 1.3 reveals that there are marked seasonal differences in ozone levels when comparing the results based on the global model calculations and the regional calculations based on ozone climatology and the Mace Head correction. For the global model calculations, and subsequently the regional nested calculations, ozone levels are markedly higher for most of the year. In the spring months (Figure 1.3b) calculated daily maximum ozone levels are on average more than 4 ppb higher over Europe. However, in summer the globally based calculated ozone levels are lower in most of Europe, and in particular so in southern Europe.

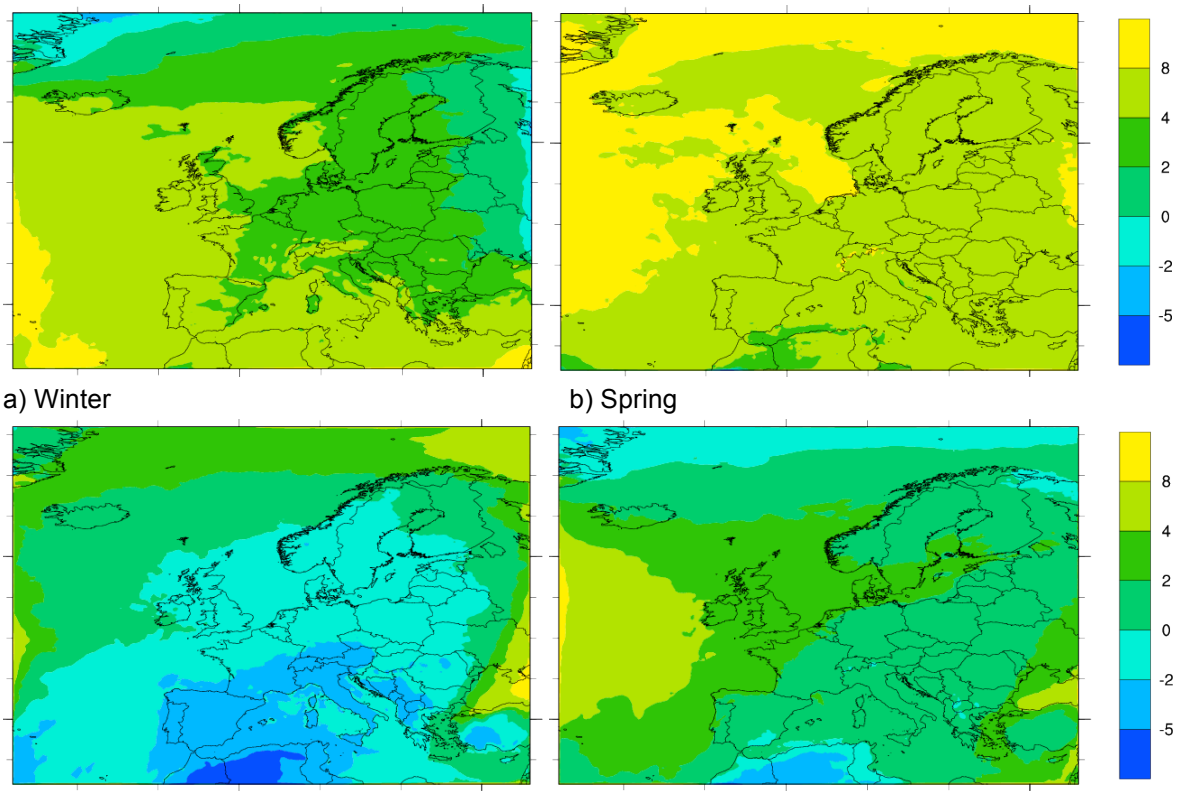

a) Winter b) Spring

c) Summer d) Autumn

Figure 1.3. *Difference for calculated daily maximum ozone in ppb between calculations nested with 6 hourly BCs from global model run and BCs with Mace Head correction.*

The differences between the regional model calculations with the Mace Head correction and global/global based calculations are also illustrated by the time series as shown in Figure 1.2. For most of the sites the measurement based regional calculation with Mace Head corrections gives the

best result. The pattern with too high ozone levels, in particular in spring, for the globally based calculations is also seen in the time series. There are small differences in model score between the global model calculations and the finer scale regional calculations with 6 hourly and monthly updated BCs. One exception is Montelibretti. This site is relatively close to Rome. The poorer performance of the global calculation here is probably caused by high emissions from Rome included in the coarse 1 x 1 degree global grid, whereas in the fine scale regional grid these emissions are better resolved horizontally.

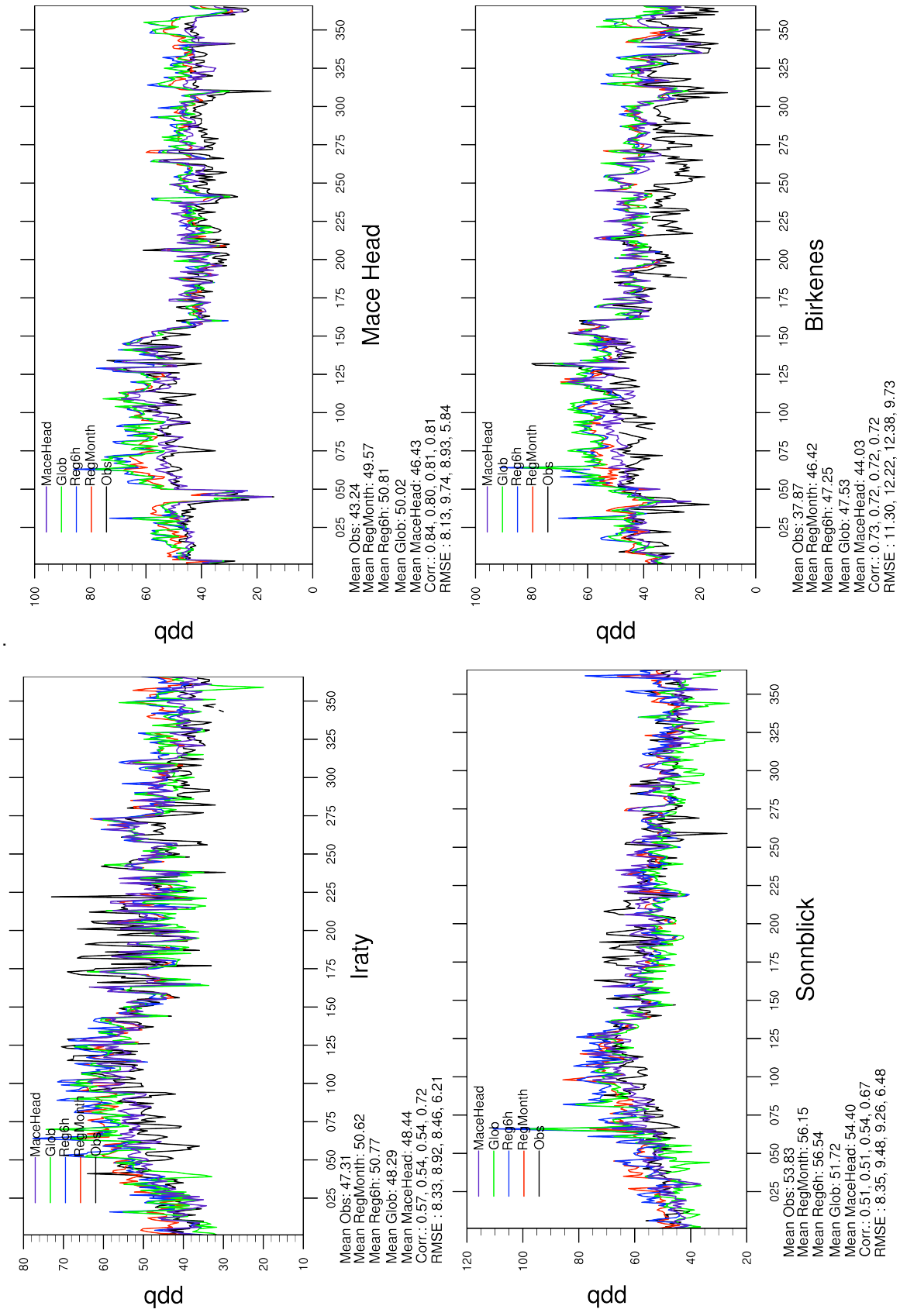

Fig. 1.3. Continued on next page.

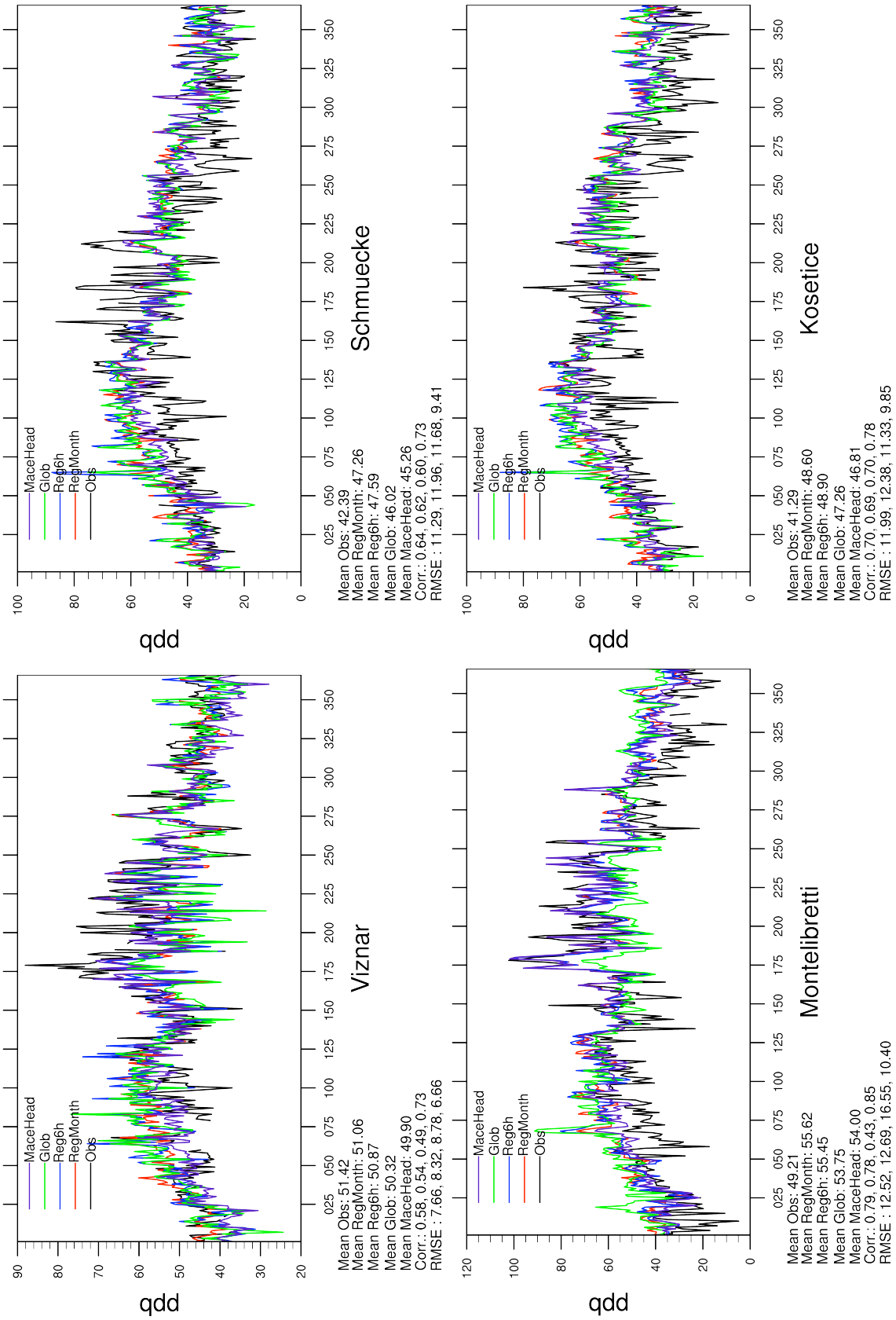

Fig. 1.3. *Continued from previous page. Timeseries for daily maximum ozone in ppb. Obs is measured concentrations. RegMonth is regional calculations with monthly updated BCs. Reg6h is regional calculations with BCs updated every 6 hours. MaceHead is regional calculations with climatology based BCs with Mace Head correction for ozone as described in Simpson et al. (2012).*

All the model runs shown here have been made with convective transport included in the calculations. The regional model runs in the main report (EMEP, 2012) are made without convective transport. We have also repeated the regional calculation with the Mace Head correction excluding convective transport with similar result as in EMEP (2012). Without convection annual mean daily maximum ozone is reduced by 2 - 4 ppb at most sites. The largest reductions, about 4 ppb, are achieved at remote coastal sites as Mace Head and Birkenes. Correlations and RMSE are also improved.

1.2. Concluding remarks

In the model calculations shown above ozone levels are overestimated. This overestimation is markedly larger than what is the case for the reference model calculations as included in EMEP (2012). As discussed above, this is caused by differences in the model setup of the regional model, as the reference model run for the EMEP report has been run without convective transport. When re-running the regional model without convection we get very similar results to what is reported in this years main report (EMEP, 2012).

A future application of nesting will be to calculate the effects future emission scenarios and/or perturbations of the emissions of air pollutants globally or from specific transcontinental regions. The calculated differences between the regional model runs using the Mace Head correction and the regional model run nested with global model calculations clearly demonstrates that the effects of the lateral boundary concentrations can be large. On the other hand the differences in model performance between the regional model runs nested with 6 hourly BSs and monthly BCs from the global model run are small, confirming the results from previous global model calculations showing only moderate predictability for transcontinental advection of ozone in the free troposphere (Jonson et al., 2010). Based on these small differences it seems likely that for most nesting applications monthly averaged lateral boundary concentrations will capture the effects of transcontinental advection of air pollutants sufficiently well.

2. Link of global and regional scale simulations of mercury

Oleg Travnikov

Given the long residence time of Hg in the atmosphere it is easily transported between continents and can significantly affect regional deposition levels. Therefore, regional scale Hg simulations largely depend on correct initial and boundary conditions (IC/BC). To provide regional simulations of the GLEMOS model with appropriate IC/BCs, the nesting procedure was developed and implemented in the model. It includes generation of IC/BCs by the global version of the model, their processing and assimilation with the regional model. The nesting procedure was tested and evaluated. Besides, a number of sensitivity runs were performed to study its principal characteristics and select the optimal parameters. Description of the nesting procedure as well as results of the sensitivity runs are given below.

2.1. Nesting procedure

Both the global and the regional versions of the GLEMOS model operate in the lat/lon projection. Configurations of the global and regional domains are shown in Fig. 2.1. The global model is applied on a regular grid with spatial resolution 1°×1°. The regional domain covers Europe and ranges from 23°E to 43°W in longitude and from 30°N to 75°N in latitude. The regional grid has spatial resolution 0.25°×0.25°. In the vertical, the global and regional grids have identical configuration of 20 non-equidistant sigma-layers. The same vertical structure allows avoiding vertical interpolation when transferring data from global to regional scale.

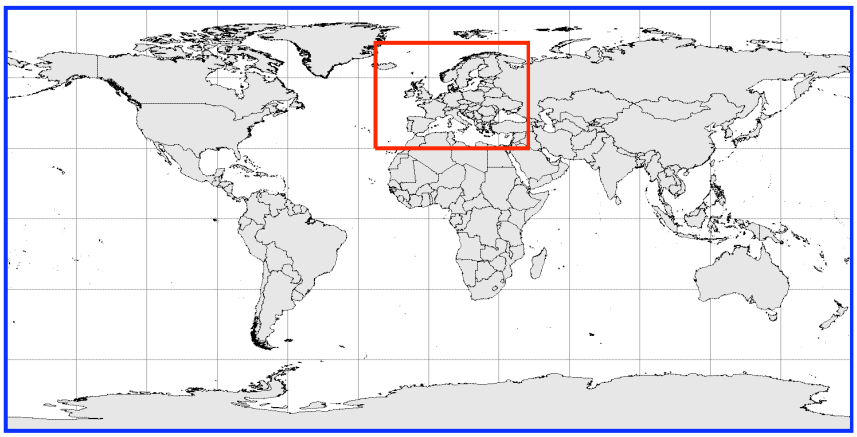

Fig. 2.1. *Configuration of the global and regional domains*

To generate IC/BCs for regional modelling 3D concentrations of three gaseous Hg species (Hg^0, Hg^{2+}, HgP) were extracted from the global scale simulation results and stored in the netCDF format. Temporal resolution of the concentration fields was 6 hours. The effect of temporal resolution of the IC/BCs on the regional simulation results was studied additionally in a series of sensitivity runs. A library of data processing routines were developed for interpolation of alternative IC/BCs generated by other models into the nested grid and assimilation by the regional version of GLEMOS.

The generated IC/BCs were used for simulation of Hg dispersion and deposition over Europe in 2009. An example of the nested simulation results is shown in Fig. 2.2. The figure presents simulated Hg deposition flux both over the global domain and over the nested regional domain. In general, the regional field reproduces the spatial pattern obtained with the global model but has much finer spatial resolution. The simulation results were evaluated against measurement data from the EMEP monitoring network in Europe. In addition, a number of sensitivity model runs were performed to test critical parameters of the nesting procedure.

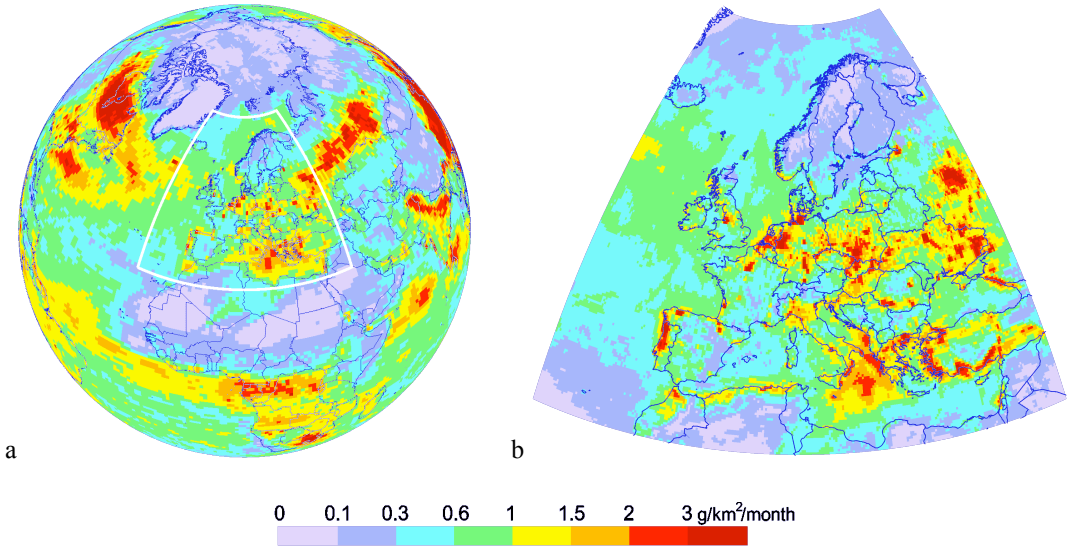

Fig. 2.2. *Spatial distribution of Hg deposition flux in January 2009 on a global scale (a) and over Europe (b)*

2.2. Sensitivity runs

The nesting procedure performance was tested in a number of model runs including the base case run and sensitivity runs. Main characteristics of the model simulations are given in Table 2.1. All tests were performed for one winter and one summer months of 2009 (January and July). The base case included a one-month spin-up with zero initial concentrations of Hg in the atmosphere and utilized boundary conditions from GLEMOS with 6 hours temporal resolution. Sensitivity runs tested the effects of the spin-up length and temporal resolution of BCs on the simulation results. In addition, we tested another set of BCs generated by ECHMERIT.

Table 2.1. *Characteristics of the model sensitivity runs*

Model runs	Spin-up length	Source of BCs	Temporal resolution of BCs	Simulation periods
Base case	1 month	GLEMOS	6 hours	Jan 09, Jul 09
# 1	15 days	GLEMOS	6 hours	Jan 09, Jul 09
# 2	1 month	GLEMOS	1 day	Jan 09, Jul 09
# 3	1 month	GLEMOS	1 month	Jan 09, Jul 09
# 4	1 month	ECHMERIT	6 hours	Jan 09, Jul 09

Simulation results of the base case model run are illustrated in Fig. 2.3. Observations of Hg0 concentration and Hg wet deposition at sites of the EMEP monitoring network are also shown for comparison. As seen the model successfully reproduces measured levels at most monitoring sites as well as spatial patterns of concentration and deposition in Europe. However, limited spatial coverage of the observations and lack of speciated Hg measurements restrict the model validation significantly.

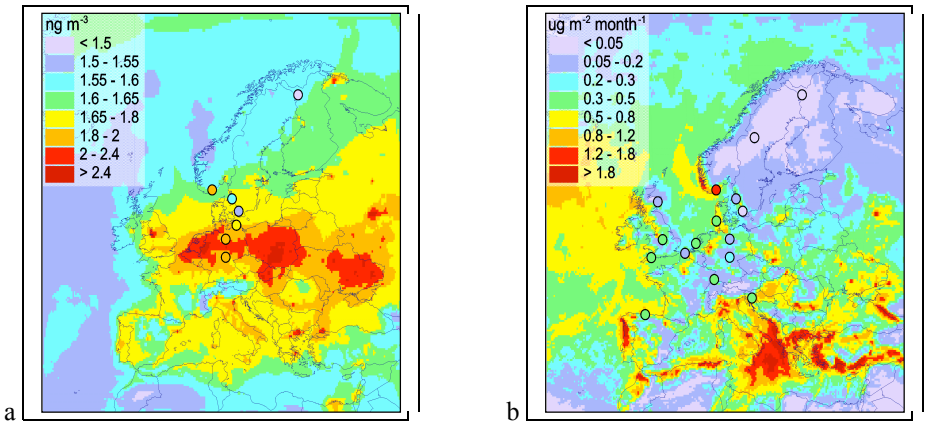

Fig. 2.3. *Simulated spatial distributions of Hg0 concentration in the surface air (a) and total Hg deposition (b) in January 2009 corresponding to the base model run. Circles show observations from the EMEP monitoring network.*

2.3. Length of spin-up

In the first set of the model sensitivity runs the effect of the model spin-up on simulation results was studied. Due to long life time of Hg in troposphere with respect to deposition, its concentration (mostly, Hg^0) is relatively evenly distributed in the vertical up to the tropopause. Therefore, it is necessary to fill the atmosphere with Hg mass to set up realistic concentrations of Hg species at the beginning of the main simulation period. We started the spin-up process with zero initial conditions and tested different spin-up lengths in terms of their effect of monthly mean simulation results. Changes of total Hg mass in the models atmospheric domain is shown in Fig. 2.4a. As seen, the model reservoir is filled within the first 15-20 days of the simulation period. After that the total mass continues growing slowly during next 20 days. Therefore, we compared the model results obtained with the 30-days and 15-days spin-up lengths (Base case and Run #1, respectively). Relative deviation of monthly mean fields of Hg species surface concentrations as well as dry and wet deposition fluxes obtained in the Run #1 from those of the base case is shown in Fig. 2.4b. In the majority of situations the difference does not exceed a few percent for all the parameters. It means that a 15-days spin-up is sufficient for monthly mean results. However, in the beginning of the simulation period the difference can be significantly bigger. Therefore, a 30-days model spin-up appears to be more appropriate for short-term simulations.

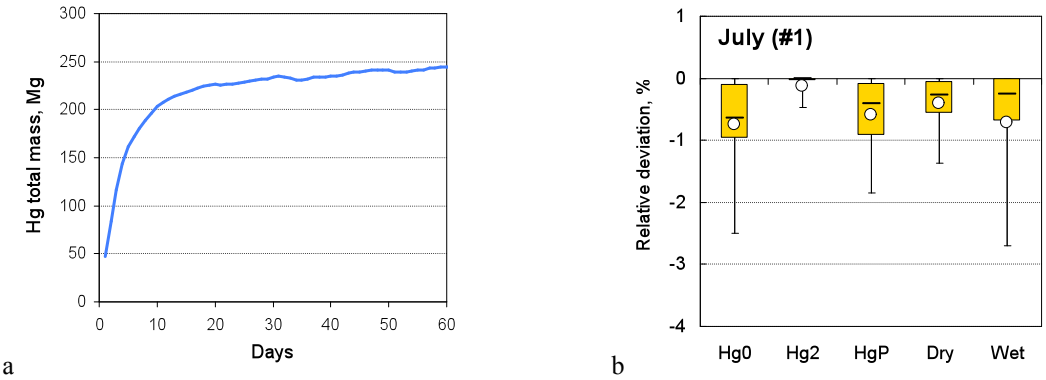

Fig. 2.4. *Temporal changes of total Hg mass in the model atmospheric domain during the model spin-up (a) and relative deviation of simulation results of Run #1 from those of the base case for July 2009 (b). The box-and-whiskers plot presents area weighted mean values (circles), medians (dash symbols), 50% variation intervals (boxes), and 90% variation intervals (whiskers).*

2.4. Temporal resolution of boundary conditions

Boundary conditions used in the base case run were assimilated with 6-hours temporal resolution. To analyse the effect of temporal resolution on modelling results we performed a number of additional sensitivity runs with daily (Run #2) and monthly (Run #3) mean BCs. The results of their comparison with the base case are shown in Figs. **2**.5 and 2.6. As seen relative difference from the base case is the smallest for Hg^0. It is below 1% both for daily and monthly BCs. Boundary conditions present well mixed background of Hg^0 in the atmosphere. Therefore, its short-term variations are relatively small and slightly affect mean Hg0 levels in the region. Temporal resolution of BCs has the largest effect on wet deposition. The relative deviation in this case is around few percents for daily BCs and up to 10-15% for monthly mean BCs. In some areas the deviation can even reach 20%. Wet deposition is more sensitive to boundary conditions, since in contrast to other parameters (surface concentrations and dry deposition) it is defined by removal from the vertical atmospheric column up to several kilometres height and it is less affected by regional emissions.

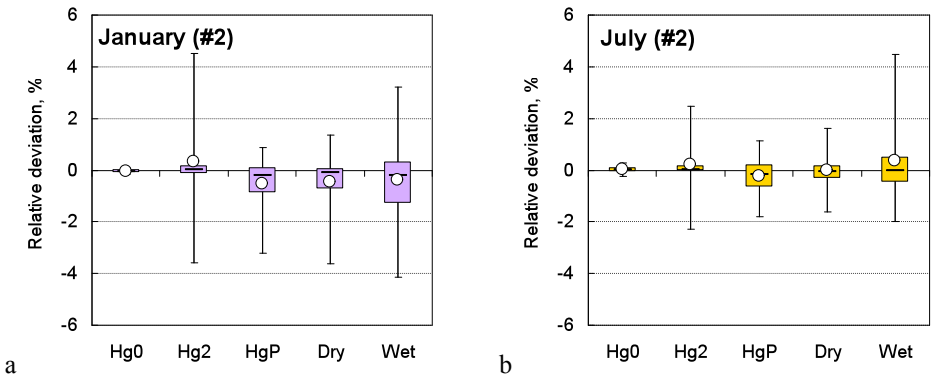

Fig. 2.5. *Relative deviation of simulation results of Run #2 from those of the base case for January 2009 (a) and July 2009 (b). The box-and-whiskers plots present area weighted mean values (circles), medians (dash symbols), 50% variation intervals (boxes), and 90% variation intervals (whiskers).*

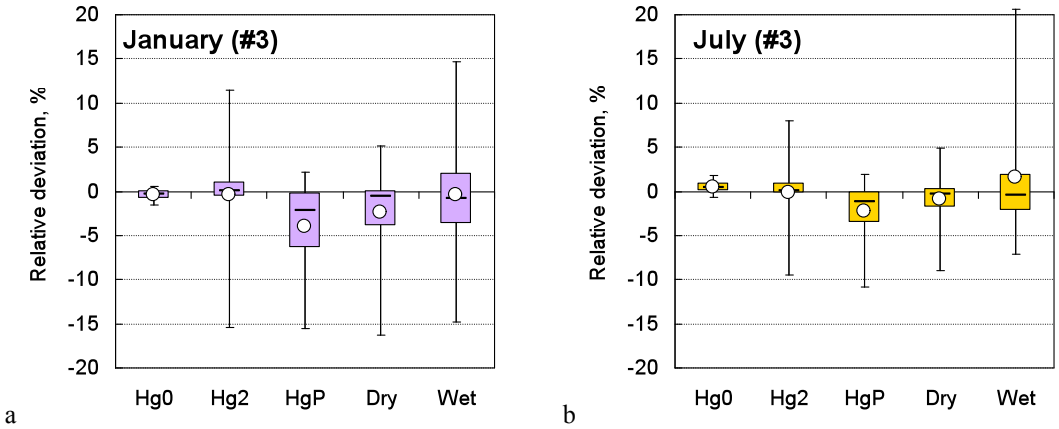

Fig. 2.6. *Relative deviation of simulation results of Run #3 from those of the base case for January 2009 (a) and July 2009 (b). The box-and-whiskers plots present area waited mean values (circles), medians (dash symbols), 50% variation intervals (boxes), and 90% variation intervals (whiskers).*

Spatial distributions of the relative deviation of wet deposition fields from Run #2 and Run #3 for January 2009 are shown in Fig. 2.7. Application of aggregated (daily or monthly) BCs leads to enhanced scavenging of oxidized Hg forms originated from boundaries over the Atlantic and, as a result, to lower wet deposition in northern Europe. Mercury deposition in Central Europe is largely

defined by regional sources and, therefore, less sensitive to boundary conditions. Thus, the difference between simulation with 6-hour, daily and monthly BCs is insignificant over the main part of continental Europe but can be noticeable over the periphery areas. Besides, the difference can be even more considerable at shorter time scales (e.g. hourly). Therefore, 6-hour BCs is a reasonable choice for simulations of short-term episodes.

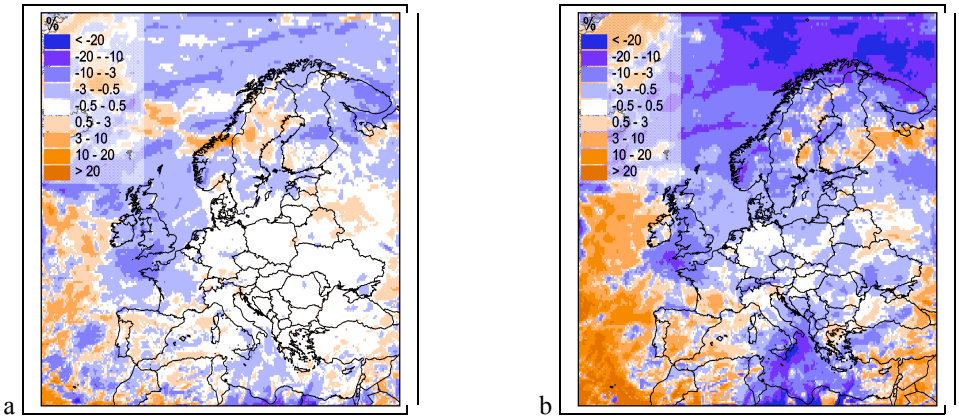

Fig. 2.7. *Spatial distribution of relative deviation of simulated Hg wet deposition obtained in Run #2 (a) and Run #3 (b) from those of the base case run for January 2009.*

2.5. Consistency of process parametrizations between model and BCs

In addition, we studied the possibility to use an alternative BC dataset generated by ECHMERIT. For this purpose, concentrations of Hg gaseous forms generated by ECHMERIT on a global scale were interpolated into the model native grid using routines from the developed data processing library and used as BCs for regional Hg simulations (Run #4). It should be noted that according to the current state of the knowledge on Hg cycling in the atmosphere, there are significant uncertainties associated with model parameterisations of Hg atmospheric chemistry and removal processes (chemical mechanisms, reaction products, removal parameters etc.) Therefore, contemporary Hg models can differ significantly in their treatment of physical and chemical mechanisms. Constrained on available scarce measurements of Hg^0 air concentration and Hg wet deposition, the models can considerably disagree in simulation of other Hg forms and dry deposition.

Deviation of the modelling results obtained with an alternative set of BCs (Run #4) from the base case is shown in Fig. 2.8. The deviation is smallest for simulated Hg0 concentration and does not exceed 10%. However, it is much higher for oxidized Hg forms (Hg^{2+} and HgP) and, as a consequence, for dry and wet deposition fluxes. In some cases the relative deviation exceeds 100-150% for these parameters.

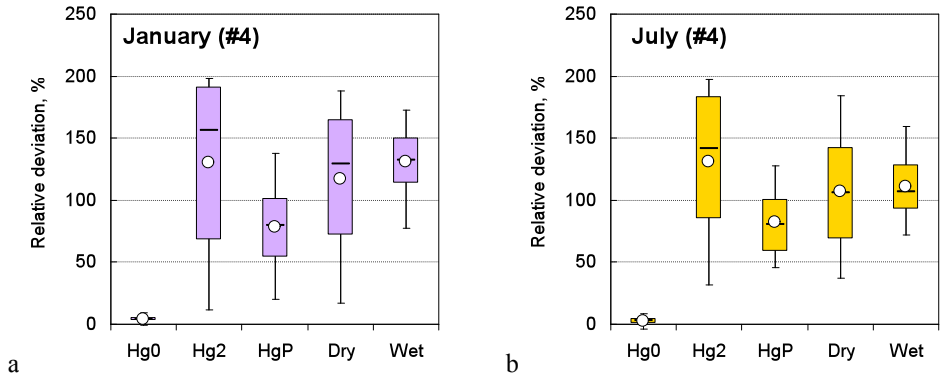

Fig. 2.8. *Relative deviation of simulation results of Run #4 from those of the base case for January 2009 (a) and July 2009 (b). The box-and-whiskers plots present area weighted mean values (circles), medians (dash symbols), 50% variation intervals (boxes), and 90% variation intervals (whiskers).*

These large deviations are the result of different treatment of Hg0 oxidation reactions products (Hg^{2+} or HgP) and removal parameters of dry and wet deposition in the ECHMERIT and GLEMOS models. The discrepancies cannot be easily resolved so far because of the lack of regular measurements of air concentration of oxidised Hg species and Hg dry deposition.

Evaluation of the simulation results obtained in the base case and in Run #4 against observations from the EMEP monitoring network is shown in Fig. 2.9. As seen the difference between two model runs is negligible for Hg0 concentration (Fig. 3.9a). Both sets of simulations well fit the measured values. However, the difference is large in the case of wet deposition (Fig. 3.9b). Results of Run #4 based on the alternative set of BCs overestimate observed wet deposition fluxes by a factor 2 or even more. Therefore, this set of boundary conditions can hardly be used for regional simulations with GLEMOS without harmonization of process descriptions between the models.

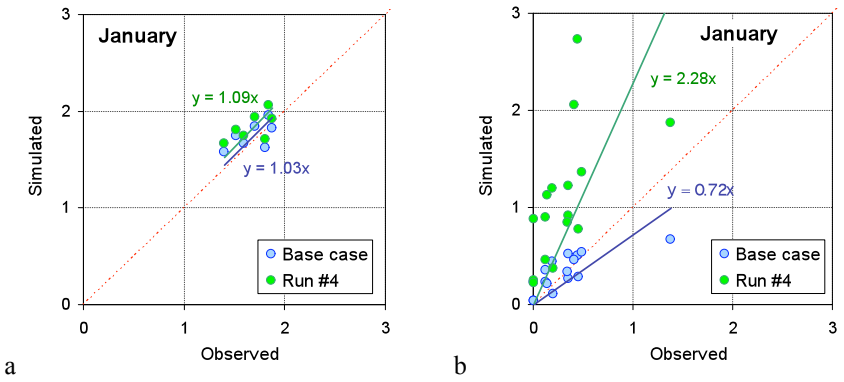

Fig. 2.9. *Comparison of simulation results for the base case and Run #4 with observations from the EMEP monitoring network: (a) – Hg0 air concentration; (b) – wet deposition flux. Red dashed line shows the 1:1 ratio.*

Thus, consistency between process parameterisations applied in a regional model and those in a global model generating BCs is critical for regional scale Hg simulations.

2.6. Concluding remarks

Three regional models of the GLEMOS model consortium (WRF-Hg, CMAQ-Hg and GLEMOS) were adapted and tested for assimilation of BCs generated by two global models (ECHMERIT and GLEMOS). Appropriate data processing routines were developed for interpolation of the original global Hg concentration fields to the native grids of the regional models. A number of sensitivity runs were performed to study effects of principal BC characteristics on the simulation results. Based on the analysis performed it can be concluded that:

- Concentrations of Hg^0 in Europe are dominated by the amount of Hg^0 transported via the boundaries into the model domain,
- Reactive mercury ($Hg^{2+}$and PHg) concentrations are significantly influenced by concentrations at the boundary but not as much as Hg^0 ,
- Local emissions have only minor effects on Hg^0 concentrations but may be regionally dominant for Hg^{2+} and PHg,
- The length of the model spin-up for Hg simulations on a regional scale should not be shorter than 30 days;
- Different temporal resolution of BCs does not affect significantly monthly mean simulation results but for simulations of short-term episodes 6-hourly BCs are recommended;
- Consistency between process parameterisations applied in a regional model and those in a global model generating BCs is critical for regional scale Hg simulations.

3. Global-scale simulations of HCB cycling in the environment

Alexey Gusev, Victor Shatalov and Valeriy Sokovykh

This section describes the progress in the evaluation of HCB pollution levels on global scale.

Theoretical investigation of HCB transport and accumulation in the environment were carried out by MSC-E for a number of recent years. The results of the investigations show the following peculiarities of HCB fate in the environment:

- high life-time in the atmosphere leading to global character of HCB pollution;
- essential influence of re-emissions of HCB on the contemporary HCB atmospheric concentrations due to HCB mass historically accumulated in the underlying surface (soil, seawater).

The data on HCB historical emissions are rather scarce and are subject to high uncertainties. To overcome this difficulty, during 2009 – 2011 MSC-E has performed the activities on the construction of HCB emission scenarios and testing them using hemispheric and regional modelling [*Gusev et al.*, 2009; *Shatalov et al.*, 2010; *Gusev et al.*, 2011].

Due to the above mentioned peculiarities of HCB fate in the environment, long-term simulations of transport and accumulation of this contaminant in the environment on global scale should be performed. In this year the first attempt of such modelling was undertaken. To do that HCB global emission data were prepared. Using these data global scale modelling of HCB cycling in the environment was performed by multi-compartment modelling system GLEMOS for the period from 1945 to 2010 with spatial resolution 3°×3°.

3.1. Emissions

Three scenarios of historical HCB emissions (maximum, average and minimal) were constructed earlier for modelling of long-term accumulation of the pollutant in the underlying surface [*Shatalov et al,.* 2010]. Preliminary calculations made with the use of GLEMOS system showed that calculation results obtained with maximum scenario agree best of all with available measurement data. Thus, this particular scenario was used in long-term global simulations with resolution 3°×3°. In modelling it was supposed that half of emissions enter to the atmosphere and other half – in soil.

According to this scenario, global HCB emissions were increasing during the period from 1945 to 1978 reaching 18 thousand tonnes in the end of the period (Fig.3.1). Further in 80th of the previous century emissions have been reduced rapidly with subsequent moderate decrease (about 10% a year on the average) beginning from 1987. Total emissions of HCB in 2010 amounted to 55.5 tonnes.

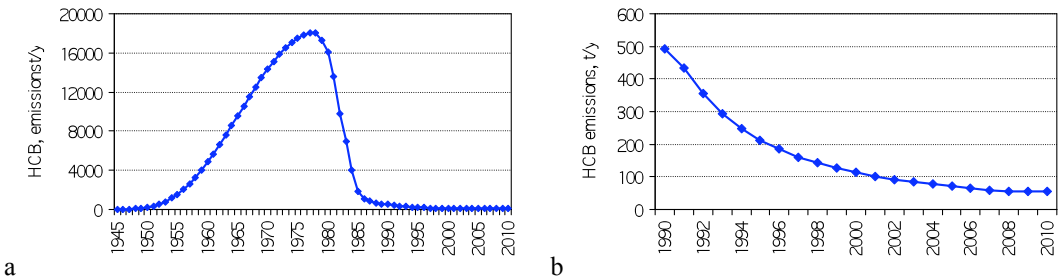

a b

Fig. 3.1. *Time trend of HCB global atmospheric emissions: 1945-2010(a), 1990-2010(b)*

Traditionally, main HCB contributors to the environmental contamination were Europe and Asia. However, the spatial pattern of contamination changed in time. Spatial distributions of emissions in

1978 (the year with maximum emissions) and in 2010 are shown in Fig. 3.2. In particular, the share of European emission sources decreased from 16.7% in 1978 to 12.5% in 2010 whereas the share of Asian sources increased from 25.6% to 50.9% during the same period.

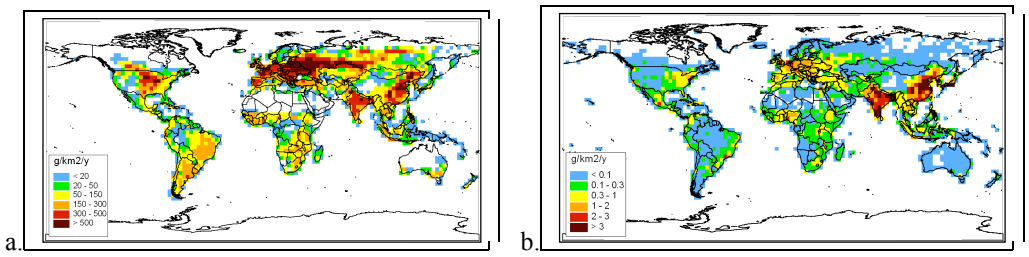

Fig. 3.2. *Spatial distribution of HCB emissions in 1978 (a) and in 2010 (b) over global domain with resolution* 3^0x3^0

3.2. Long-term accumulation in the environment

According to simulation results, the ocean contains 40-60% of total environmental content of HCB. Soil content is about 30% – 40%. The share of HCB in the atmosphere is continuously decreasing fro 30% – 35% in the end of 40th previous century to less than 1% in XXI century (Fig. 3.3).

The most part of HCB mass is removed from the environment due to ocean degradation and sedimentation (Fig. 3.4). These processes are responsible for ~70-80% of total removal in the last years. The contributions of soil degradation amount to ~15-20%. The relative importance of the removal from air decreases from 55% in 1945 to 3% in 2010.

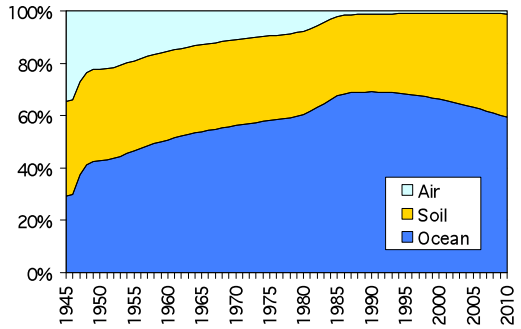

Fig. 3.3. *The percentage ratio of HCB content in environmental media for time period from 1945 to 2010*

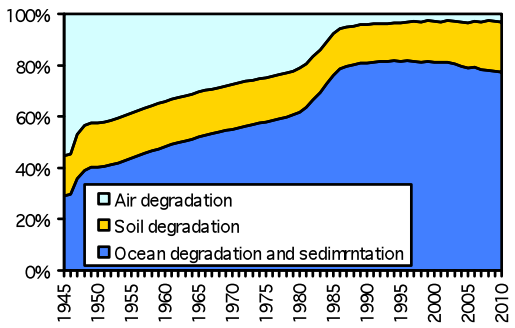

Fig. 3.4. *The percentage ratio of different ways of HCB removal from environmental media for time period from 1945 to 2010*

Annual HCB fluxes between environmental media are shown in Fig. 3.5. It is seen that the fluxes from soil to the atmosphere and from the atmosphere to ocean are prevailing. So, globally HCB mass is transported from soil to ocean through the atmosphere. In the ocean HCB is partially accumulated and partially removed from the environment via sedimentation and degradation processes.

Annual mass flux integrated over the year is always directed from soil to the atmosphere (lower curve in Fig. 3.5). However, in some particular regions this flux can have opposite direction. Spatial distribution of HCB gaseous flux from the atmosphere to soil in 1978 (the year with maximum emissions) is shown in Fig. 3.6. It can be seen that in the areas with relatively small emissions this flux is directed from the atmosphere to soil. This is particularly characteristic of high-latitude regions where HCB is intensively accumulated in soil (the effect of ***cold condensation***).

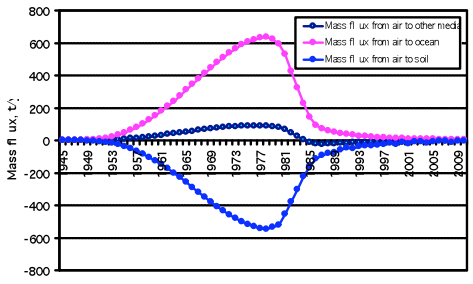

Fig. 3.5. *Time trends of HCB mass fluxes from air to other media (negative values correspond to the flux of reverse direction)*

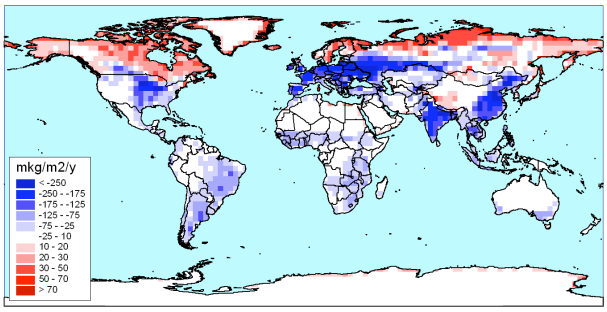

Fig. 3.6. *Spatial distribution of HCB gaseous flux from air to soil in 1978 (negative values correspond to the flux of reverse direction)*

3.3. Results for 2010

Let us consider in more detail the results of global modelling concerning the last year of the calculation period (2010).

The atmosphere. Maximum HCB concentrations (> 30 pg.m^3) in the atmosphere have been found in Europe, the Russian Federation, India and China. Outside highly contaminated regions air concentrations are close to background ones that depend on latitude. In particular, background HCB air concentrations in low and temperate latitudes of the Northern Hemisphere amount to 10-15 pg/m^3 (Fig. 3.7).

The results of modelling were compared to measurement data on HCB concentrations in air at the EMEP monitoring network. Annual mean concentrations were considered. The results are presented in Fig. 3.8.

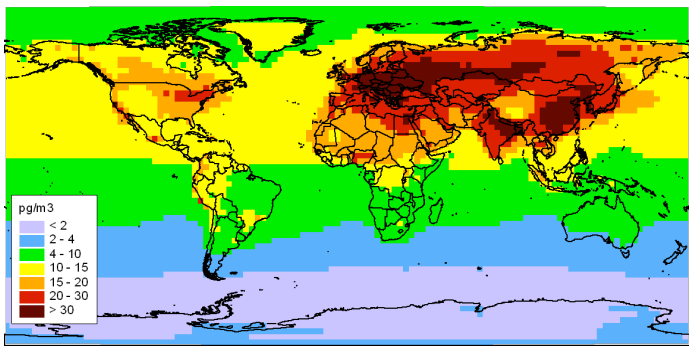

Fig. 3.7. *Spatial distributions of HCB annual mean concentration in ground air for 2010*

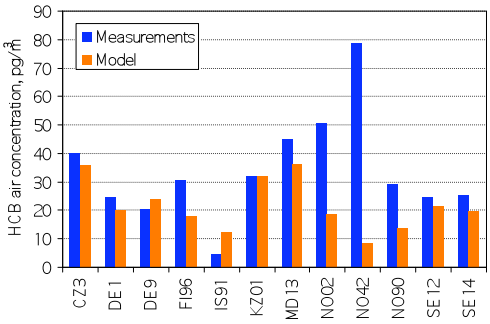

Fig. 3.8. *Annual mean HCB concentrations in air calculated by the GLEMOS model and measured at the EMEP monitoring sites in 2010*

In general, calculation results agree reasonably with measurements. About ¾ of measurements agree with calculations within a factor of two. The exceptions are Norwegian sites (particularly NO2 and NO42) where measurements essentially exceed calculated values. One of possible reasons of such disagreement may be local emission sources near Spitsbergen island (NO42) and near Skagerrak straight (NO2). This assumption can be indirectly confirmed by the comparison of measurements at *Bjornoja* (Bear Island) [*Kallenborn et al.,* 2007] located between the North Norwegian mainland and the Svalbard archipelago (Fig. 3.9) with calculated results. Air concentrations measured at this location agree well with calculation data (Fig. 3.10) being essentially lower than concentrations measured at NO2 and NO42.

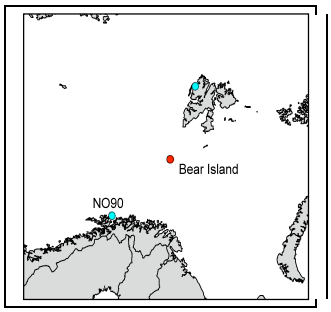

Fig. 3.9. *Relative locations of Bear Island and EMEP monitoring sites NO02 and NO42*

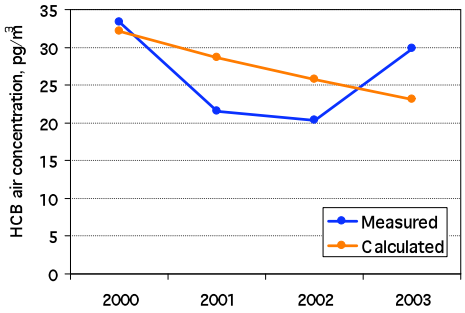

Fig . 3.10. *Annual mean HCB concentrations in air calculated by the GLEMOS model and measured at Bjornoja (Bear Island)*

Soil. Spatial pattern of HCB soil concentrations reflects the peculiarities of historical accumulation of the pollutant. Maximum contamination in soil takes place in areas with high emissions and in regions with high latitudes due to cold condensation mentioned above. Highest soil concentrations are characteristic of Europe and Russia where they exceed 50 – 100 pg/g (see Fig. 3.11).

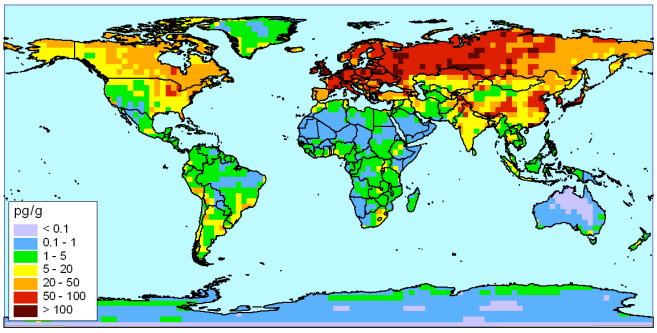

Fig. 3.11. *Spatial distributions of HCB annual mean concentration in soil for 2010*

The ocean. The distribution of HCB concentrations in surface layer of seawater is given in Fig. 3.12. There is evident latitudinal dependence of pollution level. The highest values of HCB concentrations in seawater (more then 3 pg/L) were obtained for high-latitude regions. The reason for this is strong temperature dependence of the gaseous flux from air to water: lower air temperatures correspond to higher air-water flux. Seawater HCB concentrations in the Antarctic region are higher than those in the temperate latitudes of the Southern Hemisphere.

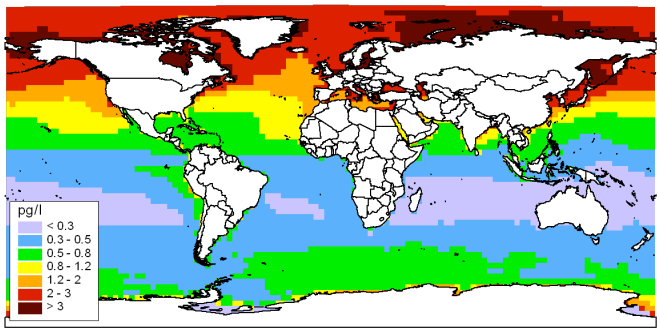

Fig. 3.12. *Spatial distributions of HCB annual mean concentration in seawater for 2010*

3.4. Concluding remarks

- The spatial pattern of HCB atmospheric concentrations is determined mainly by secondary emission sources, that is, by re-emission from HCB historically accumulated in the underlying surface. Hence, for simulations of HCB contamination levels both in the EMEP region and over the entire globe consideration of historical HCB accumulation is of particular importance.

- Emission scenario for historical and contemporary emissions worked out by MSC-E allowed obtaining reasonable agreement between calculated and measureв HCB air concentrations at the sites of EMEP monitoring network.

- Air concentrations of HCB in the regions free from emission sources (10 – 15 pg/m^3) is comparable in order of magnitude with concentration levels in contaminated regions. This is conditioned by extremely high persistence of HCB in the atmosphere.

- Among important directions of further investigation of HCB transport and accumulation in the environment the following activities should be mentioned: elaboration of vegetation module for GLEMOS modelling system, collection measurement data on contamination levels of HCB in various environmental media and usage these data for calibration of the model and refinement of emission scenarios.

4 Chemical and physical transformations of mercury in the ocean: a review

Nadezhda Batrakova, Oleg Travnikov and Olga Rozovskaya

4.1. Mercury speciation in the ocean

The ocean plays a critical role in the biogeochemical cycling of mercury (Hg). As estimated by *Mason and Sheu* [2002] ocean waters contain 1440 Mmol (2.89×10^5 Mg) of Hg, whereas the atmospheric reservoir contains 25 Mmol (5.01×10^3 Mg). Ocean emissions contribute approximately 30-40% of the current Hg source to the atmosphere [*Sunderland and Mason*, 2007; *Pirrone et al.*, 2009], which include also anthropogenic sources, evasion from soils and activities of hydrothermal vents and volcanoes. Oceanic mercury influence human health by means of bioaccumulation in fish in the form of toxic methylmercury. Nevertheless the marine biogeochemistry of Hg remains poorly understood [*Strode et al.*, 2010].

Poissant et al. [2002] classified marine environments into three compartments: coastal zones, areas of upwelling and open oceans. These zones correspond to 0.1%, 10% and 90% of the total area of the oceans respectively. Over these three zones, mercury is deposited from the atmosphere by wet and dry deposition. River systems are sources of mercury in specifically coastal zones. Upwelling and sea currents can play a significant role in mercury transport to open oceans. Reactive mercury can be transported with particles from upper layers of the ocean to deep ocean areas where oxygen content is lower [*Poissant et al.*, 2002]. Deep ocean sediments; estuarine and shelf sediments are the most likely locations of methylmercury production, but methylation of mercury can also take place in the ocean water column [*Whalin et al.*, 2007]. Mercury cycle in the ocean is schematically shown in Fig. 4.1.

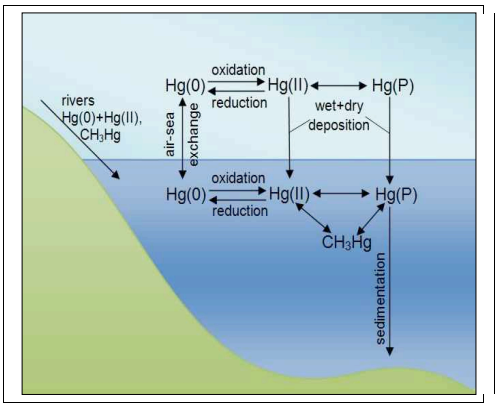

Fig. 4.1. *Mercury cycle in the ocean.*

Mercury exists in different chemical and physical forms in the ocean waters [*Hines and Brezonik,* 2004]. Bioavailability and toxicity of mercury in the ocean depend on its speciation in water [*Bloom,* 1992; *Benoit et al.*, 2001a; *Choe et al.*, 2003a; *O'Driscoll et al.*, 2003a,b].

Total mercury in the ocean include dissolved mercury species Hg(II), dissolved gaseous mercury (DGM), and particulate adsorbed mercury species Hg(P). Dissolved gaseous mercury is mainly composed of gaseous elemental mercury (GEM) in estuaries and the Surface Ocean. Elemental mercury is volatile and it is the main form of mercury found in the atmosphere, while bivalent mercury is the predominant form found in water, bound to various organic and inorganic ligands [*O'Driscoll et al.*, 2005, 2006]. DGM can also include methylmercury, dymethylmercury, and some ethylmercury, but concentrations of these forms is not significant in surface waters, however, quantity of methylated forms is relatively large at depth in the ocean [*Amyot et al.*, 1997; *Gill*, 2008, *Morel et al.*, 1998]. A list of published DGM concentrations in sea and ocean water is presented in Table 4.1.

Table 4.1. *DGM Concentrations in Seawater*

Location	Year	Hg conc.	Range	Units	Reference
North Pacific		60 ± 30		fM	*Laurier et al.*, 2003
South and equatorial Pacific Ocean		130 ± 70		fM	
South and equatorial Pacific Ocean			60 - 140	fM	*Kim and Fitzgerald,* 1986
Equatorial Pacific			50 - 225	fM	*Kim and Fitzgerald*, 1986
Equatorial Pacific			15 - 690	fM	*Mason and Fitzgerald*, 1993
Equatorial Pacific			40 - 325	fM	*Mason and Fitzgerald*, 1993
North Atlantic Ocean		410 ± 310		fM	*Mason et al.*, 1998
	1993	650 ± 390	150 - 1500	fM	*Mason et al.*, 1998
	2005	58 ± 10	28 - 89	fM	*Andersson et al.*, 2011
South Atlantic Ocean		1200 ± 800		fM	*Mason and Sullivan*, 1999
South and equatorial Atlantic Ocean			80 - 160	fM	*Mason et al.*, 2001
South and equatorial Atlantic Ocean		110		fM	*Gardfeldt et al.*, 2003
Ireland, Mace Head	1999	107		fM	*Gardfeldt et al.*, 2003
Mediterranean Sea, East	2000	170			
Mediterranean Sea, West	2000	75			
Tyrrhenian Sea	2000	95			
Mediterranean Sea, East	2000	211	201 - 221	fM	*Ferrara et al.*, 2003
Mediterranean Sea, West	2000	88	Profiles		
Mediterranean Sea, West	2000	670			
Mediterranean Sea, West			35 - 220	fM	*Cossa et al.,* 1997
Mediterranean Sea		150 ± 120		fM	*Horvat et al.*, 2003
Mediterranean Sea, West	2003	200		fM	*Andersson et al.*, 2007
Tyrrhenian Sea	2003-2004		100-300		
Ionian Sea	2003-2004		80-330		
Adriaric Sea	2004		150-210		
Adriaric Sea, North	2004		350-1030		
Mediterranean Sea, Strait of Sicily	2003-2004		100-140		
Mediterranean Sea, Strait of Messina	2003	220			
Mediterranean Sea, Strait of Otranto	2003-2004		130-180		
Mediterranean Sea	2003-2004		120-190	fM	*Andersson et al.*, 2007
North Sea	1992-1996		60-800	fM	*Baeyens and Leermakers*, 1998
	1993 - 1994	260 ± 110		fM	*Coquery and Cossa*, 1995
Baltic Sea	1997-1998	90	70 – 100	fM	*Wangberg et al.*, 2001
	2006		50-160	fM	*Kuss and Schneider*, 2007
Arctic Ocean, Beringia	2005	220 ± 110	25 – 670	fM	*Andersson et al.*, 2008
Canada, Bay St.Francois	2003		21-145	pg/L	*Zhang et al.*, 2006
Japan, Tokyo Bay	2003 - 2005	52 ± 26		ng/m^3	*Narukawa et al.*, 2006
Black Sea, CS (Coastal site)	2005		251-893	fM	*Lamborg et al.,* 2008
Black Sea, WG (Western Gyre)	2005		206-1161	fM	*Lamborg et al.*, 2008
Mediterranean Sea, Strait of Sicily	2000	90	max	pg/L	*Gardfeldt et al.*, 2003
France, Arcachon Bay, Aquitaine	2005 - 2007	50 ± 42	5 – 193	pg/L	*Bouchet et al.,* 2011
USA , Chesapeake Bay	1997		20 - 60	pg/L	*Mason et al.*, 1999
USA, San Francisco Bay	1999 - 2000	181 ± 177		pg/L	*Conaway et al.*, 2003
Brazil, Sepetiba Bay			32 - 82	pg/L	*Boszke et al.*, 2002
	2001 - 2002		10 - 110	pg/L	*Molisani et al.*, 2007
Global ocean (modelling)		70		fM	*Strode et al.*, 2007

Many investigations have demonstrated differences in mercury concentrations among ocean basins [*Laurier et al*., 2004; *Mason and Gill*, 2005]. For instance, on average the Atlantic Ocean [*Dalziel,* 1995; *Mason et al*., 1998; *Mason and Sullivan*, 1999] mercury concentrations are higher than in the Pacific Ocean [*Gill and Fitzgerald*, 1988; *Laurier et al*., 2004; *Mason and Fitzgerald*, 1991,1993] but lower than in the Mediterranean Sea [*Cossa et al*., 1997,2004; *Sunderland*, 2007]. Concentration values of total mercury in coastal waters and in the open ocean are in the order of 10^{-12} M [*Sunderland and Mason*, 2007; *Gill*, 2008]. A list of published total mercury concentrations in sea and ocean water is given in Table 4.2. Total mercury concentrations average from 1 to 10 pM whereas concentrations of dissolved gaseous mercury are ranged from 50 to 250 fM. In general, concentrations of Hg(0) are higher near the air-water interface whereas levels of methylmercury are higher near the sediments [*Morel et al*., 1998].

Table 4.2. *Total Mercury Concentrations in Seawater*

Location	Year	Hg conc.	Range	Units	Reference
North Atlantic Ocean		2.4 ± 1.6		pM	*Mason et al*., 1998
Deep North Atlantic Ocean		2.3 ± 0.8		pM	*Mason et al*., 1998
South and equatorial Atlantic Ocean		1.68 ± 0.74		pM	*Mason and Sullivan,* 1999
South and equatorial Atlantic Ocean		2.9 ± 1.7		pM	*Mason and Sullivan*, 1999
North Atlantic, Celtic Sea, LDW (lower deep water)	1994 - 1995	1.96 ± 0.23	Profiles	pM	*Cossa et al.,* 2004
North Atlantic, Celtic Sea, LSW (Labrador sea water)	1994 - 1995	1.97 ± 0.63	Profiles	pM	
North Atlantic, Celtic Sea, MIW (Mediterranean intermediate water)	1994 - 1995	2.04 ± 0.84	Profiles	pM	
North Atlantic, Celtic Sea, ISOW (Iceland-Scotland overflow water)	1994 - 1995	2.76 ± 0.35	Profiles	pM	
North Atlantic, Celtic Sea	1994 - 1995	2.1 ± 0.6		pM	*Cossa et al*., 2004
North Atlantic (Mediterranean Sea)		1.57 ± 0.44		pM	*Cossa et al.,* 1997
Gibraltar, MOW (Mediterranean outflow water)		2.23 ± 0.41		pM	*Cossa et al.,* 1997
Mediterranean Sea, West		2.54 ± 1.25		pM	*Cossa et al*., 1997
		1.46 ± 0.41		pM	*Horvat et al*., 2003
			1.72 - 1.93	pM	*Horvat et al*., 2003
North Pacific		0.64 ± 0.26		pM	*Laurier et al*., 2004
Black Sea, CS (Coastal site)	2005		1.6-7.6	pM	*Lamborg et al*., 2008
Black Sea, WG (Western Gyre)	2005		1.9-11.8	pM	

Bivalent mercury (Hg(II)) is a relatively reactive species in the environment. In seawaters the bivalent mercury is not present as the free ion, it present mainly as inorganic and organic complexes. The concentration of the free metal ion (Hg^{2+}) is exceedingly small in seawater systems ($<1\cdot10^{-18}$ M) [*Mason and Fitzgerald*, 1996]. Consequently, the level to which Hg may transform between its different oxidation states, and forms, is defined by the reactivity of the inorganic and organic complexes of bivalent mercury [*Whalin et al*., 2007].

As showed by *Morel et al*. [1998], in natural aquatic systems inorganic complexes of Hg (II) include complexes with variable amounts of hydroxide ($Hg(OH)^+$, $Hg(OH)_2$, $Hg(OH)_3^-$), and of chloride ($HgCl^+$, $HgCl(OH)$, $HgCl_2$, $HgCl_3^-$, $HgCl_4^{2-}$) ions depending on the pH and the chloride concentration. For seawaters the most typical complexes are $HgCl_3^-$, $HgCl_4^{2-}$. Complexes with bromide ions are also significant in seawater. $Hg(OH)_2$ is the weakest of the known dissolved complexes of mercury. Slightly stronger are complexes with halides - chloride and bromide. Stronger complexes are formed with organic matter and sulfides. Even in oxic surface waters, some of Hg(II) may be bound to sulfides (S^{2-} and HS^-), which have been measured at nanomolar concentrations in surface seawater [*Luther et al.,* 1989; *Morel and Hering*, 1993; *Morel et al*., 1998; *Whalin*, 2005]. Among organic complexes of Hg(II) most prevalent are complexes with humic acids. The reactions of ionic mercury are relatively fast, and it is thought that the various species of Hg(II), including those in the particulate phase, are at

equilibrium with each other. Complexation with particulate matter can lead to storage of the metal if it is incorporated into the structure, or reactions may continue if the complex is surficial [*Morel et al.,* 1998; *Whalin*, 2005].

Primarily, inorganic mercury in seawater occur as Hg(II), but bivalent mercury can be reduced to elemental mercury Hg(0). Concentrations of dissolved Hg(0) are very small in seawater. Complexes of mercury in the intermediate oxidation state Hg(I) are not stable, excepting the dimer Hg_2^{2+}, but its concentration in seawater inappreciable [*Morel et al*.,1998; *Whalin et al*., 2007].

In addition to the redox transformations, Hg(II) can be taken up by microorganisms, some of which methylate the Hg(II) complexes, forming methylmercury ($CH_3Hg(II)$), in which the oxidation state of Hg is still Hg(II). In the organometallic species of mercury, the carbon-to-metal bonds are stable in water because they are partly covalent and the hydrolysis reaction, which is thermodynamically favorable (and makes the organometallic species of most other metals unstable), is kinetically hindered. As a result, the dimethylmercury species, $(CH_3)_2Hg$ is unreactive. The monomethylmercury species, CH_3Hg, is usually present as chloro- and hydroxocomplexes (CH_3HgCl and CH_3HgOH) in oxic waters [*Morel et al.,* 1998; *Whalin et al.*, 2007]. Methylmercury rather than inorganic mercury is bioconcentrated because it is better retained by organisms at various levels in the food chain. Relative efficiency of the methylation and demethylation processes control the methylmercury concentration in water, and so determine the concentration of mercury in the biota. Anoxic waters and sediments are an important source of methylmercury in the ocean, because of the methylating ability of sulfatereducing bacteria. Methylmercury may be transported from anoxic layers to surface waters. Also, methylmercury may be formed in the surface waters through biological or chemical processes. Demethylation is effected both photochemically and biologically [*Morel et al*., 1998].

Ocean cycle of mercury influences the global distribution of mercury. In particular, volatilization of DGM from water is a significant process in the global cycle of mercury. *Mason et al.* [1994] showed the importance of mercury volatilization from the ocean surface. More recently, the re-deposition of reactive mercury species were measured [*Mason et al.*, 1994, 2001]. *O'Driscoll et al*. [2003a] showed that these predictive models of mercury volatilization from water are largely governed by the wind speed and the concentration of DGM in the surface water [*O'Driscoll et al.*, 2006].

4.2. Mercury Reduction and Oxidation Processes in the Ocean

Redox reactions of mercury are significant parts of mercury cycle in the ocean (see Fig. 1). Reduction results in the production of dissolved elemental mercury Hg(0) from bivalent forms of mercury. Then this dissolved elemental mercury Hg(0) can volatilize to the atmosphere removing mercury from the Ocean. This process is facilitated by wind and surface layer disturbances [*O'Driscoll et al*., 2003a,b; *Orihel et al*., 2007; *Vost et al.*, 2012]. Reduction of mercury can be both photochemical [*Amyot et al.,* 1994; *Zhang and Lindberg*, 2001; *Amyot et al.*, 2004] and biotic [*Mason et al.*, 1995; *Siciliano et al.*, 2002].

Not all bivalent mercury Hg(II) in natural waters is present in an easily reducible form [*Strode et al.,* 2007]. *O'Driscoll et al*. [2006] estimated that reducible mercury in freshwater lakes accounted for about 40% of the total mercury. One of hypotheses that in order for mercury reduction to occur, Hg(II) must be complexed with dissolved organic matter (DOM); and then reduction occur by way of electron transfer from the organic ligand to mercury [*Allard et al*., 1991; *Gårdfeldt and Jonsson*, 2003; *Spokes and Liss*, 1995]. This process is inhibited in the presence of ligands such as chlorides that may compete with organic matter for binding with mercury [*Allard et al*., 1991].The size of reducible fraction is dependent on the incident wavelengths and the intensity of radiation. The most important types of radiation for mercury redox reactions are Ultraviolet A (UV-A), which characterizes by wavelength ranged from 315 to 400 nm, and Ultraviolet B (UV-B) with wavelength 280-315 nm. Under UV-B radiation more mercury is in reducible form in comparison with UV-A radiation; and under higher intensities more reducible mercury is observed likely up to an intensity maximum [*Qureshi et al.,* 2010].

The oxidation of Hg(0) is one of the least understood parts in the mercury biogeochemical cycle. Oxidation decreases concentration of dissolved gaseous mercury in aquatic environments and increases the concentration of bivalent mercury, which is the substrate for methylation [*Lin et al.*, 2012]. Oxidation of elemental mercury also can be both photochemical [*Voughan and Blough,* 1998; *Lalonde et al.,* 2001; 2004] and biotic [*Siciliano et al.*, 2002].

Mercury oxidation process can result in the formation bivalent mercury species which then could be reduced [*Whalin and Mason*, 2006; *Whalin et al.*, 2007]. Some investigators assume that mercury oxidation also can result in production of nonreducible form of bivalent mercury, which would imply that mercury redox reactions follows a three-species pathway [*Qureshi et al*., 2010] rather than a two-species pathway as has often been regarded [*Whalin and Mason*, 2006; *Whalin et al*., 2007].

4.2.1. Photochemical redox processes

4.2.1.1. Photochemical reduction

Photochemical reduction processes are characterized by high reduction rates which are in positive correlation with solar irradiance [*Whalin*, 2005]. For example, in experiments by *Amyot et al.* [1994; 2000] a positive correlation was found between production of dissolved gaseous mercury and level of UV radiation. Furthermore, maximum evasion of Hg(0) over both seawater and river surfaces was observed during daylight hours [*Gardfeldt et al*., 2001; *Whalin et al*., 2007].

Reductants

Many experiments showed that Hg(II) reduction in natural waters is correlated with content of dissolved organic matter [*Allard and Arsenie*, 1991; *Xiao et al*., 1995; *Costa and Liss*, 1999]. This DOM can act in a photosensitizing manner because it contains chromophores which can absorb light and each absorbed photon can initiate reactions [*Spokes and Liss*, 1995; *Whalin et al.*, 2005, 2007].

Bivalent mercury forms strong complexes with DOM/DOC (DOC - dissolved organic carbon). The value of the stability constants (given as log K) for these complexes are estimated from 10.6 [*Benoit, et al.,* 2001b] to 24 [*Lamborg et al.* 2002]. If the latter is correct, the majority of Hg(II) in both freshwater and coastal seawater will be organically complexed [*Spokes and Liss*, 1995; *Whalin*, 2005].

There are two hypothesized mechanisms regarding the correlation between DOM and mercury reduction [*Whalin et al*., 2007]. First is ligand metal charge transfer by chromophoric material, in other words, the direct reduction of Hg(I) or Hg(II) [*Allard and Arsenie*, 1991; *Spokes and Liss*, 1995]. Second is the formation of reactive intermediate reductants, such as $HO_2^{\bullet}$, which are formed through photolysis of DOM [*Voelker et al*., 1997; *Zhang and Lindberg*, 2001]. *Gårdfeldt et al*. [2003] however concluded that this mechanism is impossible under natural conditions and that the likely reaction mechanism for reduction is the process occurred through charge transfer.

Reduction process and rate constants

Qureshi et al. [2010] assumed that if dissolved organic matter is supposed to be the main reductant then mercury reduction may be dependent on both the nature and the total amount of DOM available in the ocean water. The nature of DOM could be estimated by observing the DOM fluorescence. Changes in DOM characteristics were not significant under UV-B radiation [*O'Driscoll et al.*, 2006; *Lepane et al*., 2003], and under UV-B radiation pseudo first order kinetics are valid. Changes in DOM composition under UV-A radiation are suggested by decreasing in DOM fluorescence [*O'Driscoll et al*., 2006]. However, experiments showed that it is unclear if and to what extent changes in DOM structure will influence the rate kinetics, and results of these experiments confirmed that first order kinetics in natural waters is correct [*O'Driscoll et al*., 2006; *Whalin and Mason*, 2006].

DOM concentration in ocean water (order of 40–100 μM [*Ogawa and Tanoue*, 2003]) is greatly higher than concentration of total mercury (order of 1–10 pM [*Mason et al*., 2001]). *Qureshi et al*. [2010] assumed that it is unlikely that DOM is a limiting factor in these experiments, even after considering that possibly not all of this 40–100 μM DOM would be involved in mercury reduction. Consequently, if dissolved organic matter is supposed to be the main reductant, pseudofirst order kinetics can be applied for the reduction reaction.

As showed by *O'Driscoll et al.* [2006] DGM production in natural waters can be described in the following equation:

$$Hg_{reducible} + photo\text{-}reductants \leftrightarrow Hg(0) + photo\text{-}oxidants$$

This equation is often used in the elementary reaction method of reduction rate constant determination. A list of published photoreduction rate constants in seawaters is presented in Table 4.3. Photochemical reduction rate constants ranged from 1.0×10^{-7} s^{-1} to 12.0×10^{-4} s^{-1}.

Table 4.3. *Photochemical reduction rate constants of Mercury in seawater*

Location	Rate constants, s^{-1}	Comments	Sources
Baie Saint-Paul	1.6×10^{-4}	0.4 w m^{-2} UVB	*Lalonde et al.* [2001]
Patuxent River, and Brigantine Island	12.0×10^{-4}	240 w m^{-2} Visible	*Whalin and Mason* [2006]
Chesapeake Bay	6.5×10^{-4}	240 w m^{-2} Visible	*Bash and Cooter* [2008]
Chesapeake Bay	$(4.3 \pm 1.1) \times 10^{-4}$	Natural light Rate constants determined for isotope ^{202}Hg	*Whalin et al.* [2007]
Chesapeake Bay	$(8.7 \pm 4.0) \times 10^{-4}$	Natural light Rate constants determined for isotope ^{199}Hg	*Whalin et al.* [2007]
Chesapeake Bay, estuarine waters	$(6.5 \pm 2.6) \times 10^{-4}$	Midday sun	*Whalin et al.* [2007]
Chesapeake Bay, coastal waters	$(6.5 \pm 1.5) \times 10^{-4}$	Midday sun	*Whalin et al.* [2007]
Chesapeake Bay, coastal shelf waters	$(0.29 - 3.7) \times 10^{-5}$	Surface waters, May 2005	*Whalin et al.* [2007]
	$(0.067 - 0.18) \times 10^{-5}$	Deep waters, May 2005	
	$(0.1 - 29) \times 10^{-5}$	Surface waters, July 2005	
Open Atlantic Ocean (41°51′N, 60° 46′W) at a depth of 3 m below the surface	$(0.42\text{-}2.58) \times 10^{-4}$	0.15 UV-A; 0.4-0.9 UV-B	*Qureshi et al.* [2010]
Used for modelling	*min*: $<1.0 \times 10^{-7}$ *max*: 8.7×10^{-4}		*Soerensen et al.* [2010]

For describing mercury redox processes the most researchers use two-species pathway which include two forms of mercury (Hg(0) and Hg(II)) as parts of redox reactions, and mercury reduction-oxidation as a simple reversible reaction.

Qureshi et al. [2010] disprove assumption that mercury reduction-oxidation is a simple reversible reaction, because in their experiments DGM concentrations didn't increase exponentially to a maximum and then stay at this maximum value thereafter. Concentration of DGM in these experiments reached a maximum usually within 1-5 h, and then decreased with time to a nonzero value after 24 h of irradiation. So, these results indicate that mercury reduction and oxidation in ocean water is not a simple two-species reversible reaction. *Qureshi et al*. [2010] proposed that along with Hg(0) and Hg(II) new mercury species Hg* different from the reducible form of mercury $Hg_r(II)$ is involved in mercury redox reactions. Hg* is produced by oxidation of Hg(0).

Hereunder, *Qureshi et al.* [2010] proposed two alternative reaction pathways involving Hg* that can be written as follows.

Pathway (I):

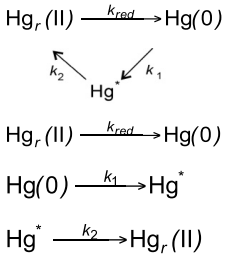

$$Hg_r(II) \xrightarrow{k_{red}} Hg(0)$$

$$Hg(0) \xrightarrow{k_1} Hg^*$$

$$Hg^* \xrightarrow{k_2} Hg_r(II)$$

where k_1 is the rate constant for conversion of Hg(0) to Hg* and k_2 is the rate constant for conversion of Hg* to Hg_r(II).

Pathway (II):

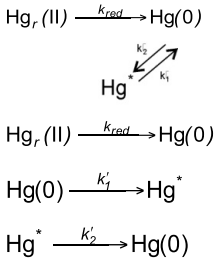

$$Hg_r(II) \xrightarrow{k_{red}} Hg(0)$$

$$Hg(0) \xrightarrow{k_1'} Hg^*$$

$$Hg^* \xrightarrow{k_2'} Hg(0)$$

where k_1' is the rate constant for conversion of Hg(0) to Hg* and k_2' is the rate constant for conversion of Hg* to Hg(0).

For all samples and radiation intensities it was found that k_1 or $k_1' > k_{red} > k_2$ or k_2'. The presence or absence of microbes and colloidal phase did not influence mercury oxidation kinetics appreciably [*Qureshi et al*., 2010]. It was also found that it is not possible to decide which of pathways (I) or (II) provides a better description of the observations. Sensitivity analysis showed that the most important parameter, which influence predicted concentration of DGM, is the rate constant measured in dark conditions. Three-species pathways described by *Qureshi et al.* [2010] may be perspective for further investigating of mercury redox chemistry. However, a two-species pathway has often been considered as appropriate pathway for describing of mercury redox processes.

4.2.1.2. Photochemical Oxidation

Mercury reduction process is described long ago, whereas process of mercury oxidation was considered to be a negligible process, based on an assumed "unreactive" nature of Hg(0). However, recent investigations (e.g. by *Whalin et al.* [2007]) showed that oxidation process occurs in the waters of different sites and that the rate constants for mercury oxidation are on the same order of magnitude as those for reduction. Rate of oxidation reactions are higher under solar irradiation.

Oxidants

Many studies suggest that the dominant oxidant of mercury in natural waters is hydroxyl radical ($OH^{\bullet}$) [*Gardfeldt et al*., 2001; *Hines and Brezonik*, 2004] which is produced, for instance, by photolysis of nitrate/nitrite [*Voughan and Blough*, 1998] or Fe(III)-organic acid coordination compounds [*Zhang and Lindberg,* 2001].

Some investigators assumed that halides, such as chloride and bromide, also may be oxidants of Hg(0) in natural waters [*Mason et al*., 2001; *Lalonde et al*., 2001; *Hines and Brezonik*, 2004], and various mechanisms have been hypothesized. The first is occurrence of the halides (chloride or bromide) reaction with $OH^{\bullet}$, which results in formation of the additional oxidants, such as OCl^{-}, OBr^{-} or Br_2^{-} [*Zafiriou et al*., 1987; *Whalin et al*., 2007]. Experiments have shown that this mechanism potentially occurs in simple artificial solutions [*Mason et al*., 2001], but it unlikely occurs in natural waters. Nevertheless, this mechanism is assumed to be acceptable for Hg(0) oxidation in the aqueous solutions of the marine atmosphere [*Lin and Pehkonen*, 1999]. The other proposed mechanism is formation of stable complexes of halides with Hg ions, Hg(I) and Hg(II), which results in decrease of the reduction and so contributing to greater net oxidation [*Whalin et al*., 2007].

Lalonde et al. [2004] suggested that Hg(0) oxidation appears to be carried out also by organic acids such as semiquinones in artificial saline waters.

Oxidation Process and Rate Constants

Qureshi et al. [2010] assumed that if hydroxyl radical is supposed to be the main oxidant of mercury then mercury oxidation process may be dependent on availability and concentration of $OH^{\bullet}$ radical. Concentration of $OH^{\bullet}$ radical in seawater is estimated at the order of 10^{-17} –10^{-18} M [*Mopper and Zhou*, 1990], and it can be accepted to be constant [*Liu et al.,* 2007]. This concentration is lower than the concentration of mercury in the ocean water. Rates of $OH^{\bullet}$ production are estimated to be about 10 nM h^{-1} (0.24 μM d^{-1}) in the open ocean surface water and about 100 nM h^{-1} (2.4 μM d^{-1}) in coastal surface water [*Mopper and Zhou*, 1990]. Thus, supply of hydroxyl radicals is much more intensive than the concentration of total mercury in the ocean water, and, therefore, pseudo first order kinetics can be applied for the oxidation reaction as well as for reduction reaction [*Qureshi et al*., 2010].

Hg(0) oxidation in natural waters can be described in the following equations [*Whalin et al*., 2005]:

$$Hg(0) \xrightarrow{k_{ox}} Hg(II)$$

$$\frac{d[Hg(0)]}{dt} = -k_{ox}[Hg(0)]$$

$$Ln\frac{[Hg(0)]}{[Hg(0)]_0} = -k_{ox}t$$

These equations are often used in the elementary reaction method of oxidation rate constant determination. A list of published photochemical oxidation rate constants in seawaters is presented in Table 4.4. Photooxidation rate constants ranged from 5.6×10^{-6} s^{-1} to 9.7×10^{-4} s^{-1}. According to these data, the rate of oxidation was equal to or greater than that of reduction in marine water.

Table 4.4. *Photochemical oxidation rate constants of Mercury in seawater*

Location	Rate constants, s^{-1}	Comments	Sources
Baie Saint-Paul	$(1.9 \pm 0.28) \times\cdot 10^{-4}$	0.49 w·m^{-2} UV-B	*Lalonde et al*. [2001]
Patuxent River, and Brigantine Island	7.0×10^{-4}	240 w m^{-2} *Visible*	*Whalin and Mason* [2006]
Chesapeake Bay	7.2×10^{-4}	240 w m^{-2} Visible	*Bash and Cooter* [2008]
Chesapeake Bay	$(4.7 \pm 1.2) \times 10^{-4}$	Natural light Rate constants determined for isotope ^{202}Hg	*Whalin et al*. [2007]
Chesapeake Bay	$(9.7 \pm 4.5) \times 10^{-4}$	Natural light Rate constants determined for isotope ^{199}Hg	*Whalin et al*. [2007]
Chesapeake Bay, estuarine waters	$(7.2 \pm 2.9) \times 10^{-4}$	Midday sun	*Whalin et al*. [2007]
Chesapeake Bay, coastal waters	$(4.1 \pm 0.89) \times 10^{-4}$	Midday sun	*Whalin et al*. [2007]
Coastal waters of the Gulf of Mexico	$(0.25 - 0.28) \times 10^{-4}$	Natural light	*Amyot et al.* [1997]
Open Atlantic Ocean (41°51′N, 60° 46′W) at a depth of 3 m below the surface	$(1.11 - 5.28) \times 10^{-4}$	UV-A and UV-B	*Qureshi et al*. [2010]
Used for modelling	min: 5.6×10^{-6} s^{-1} max: 9.7×10^{-4} s^{-1}		*Soerensen et al*. [2010]

The rate constant for mercury oxidation in marine water is greater relative to that in freshwater [*Whalin et al*., 2007; *Lalonde et al*., 2001; *Lalonde et al*., 2004; *Soerensen et al*., 2010], perhaps by reason of producing aqueous halogen radicals, which are additional oxidants, through the reaction of hydroxyl radicals with halides (Cl^- and Br^-) [*Zafiriou et al.*, 1987], or by reason of the formation in marine water of stable Hg(II) complexes which decrease reduction rates and resulting in greater net oxidation [*Whalin et al.,* 2007; *Soerensen et al*., 2010].

It must be noted, that halogen ions, which are contained in high concentrations in the ocean, are very important for mercury chemistry in the ocean water, because these ions may be ligands for mercury

as well as photoreactants. *Lalonde et al.* [2001] and *Qureshi et al.* [2010] assume that presence of chloride ions contributes to stabilizing mercury ions in solution after the oxidation process, however, they believe that chloride ions are not an oxidant of Hg(0).

4.2.1.3. Influence of Radiation on Photochemical redox reactions

Photochemical processes could be divided into three steps: (i) absorption of radiation of certain wavelengths resulting in the formation of an excited state, (ii) primary photo-chemical processes involving the transformation of the electronically excited state and its de-excitation; and (iii) secondary or ''dark'' reactions of the various species that have been produced by the primary photochemical processes [*Bonzongo and Donkor*, 2003]. Similar to other photochemical processes, the rate of photochemical redox reactions of mercury is also observed to be dependent on the intensity and type of radiation [*Bash and Cooter*, 2008; *Qureshi et al*., 2010].

Bash and Cooter [2008] and *O'Driscoll et al.* [2006] proposed that redox rates in surface waters could be calculated taking account of radiation intensity through the following equation:

$$k(\lambda) = k_{ref} \frac{I(\lambda)}{I(\lambda)_{ref}},$$

where $k(\lambda)$ is the photoreduction or photooxidation rate as a function of radiation intentsity $I(\lambda)$ at the wavelength λ; k_{ref} is the reference rate reported in the literature and $I(\lambda)_{ref}$ is the radiation intensity of the measurement of k_{ref}.

Soerensen et al. [2010] estimated that rate coefficients in mercury photochemical redox reactions could be calculated within observational confidence limits by the following equations, which are obtained on the basis of data reported by *Qureshi et al*. [2010]:

$$k_{red}\ (s^{-1}) = 1.7 \times 10^{-6} \cdot I,$$

$$k_{ox}\ (s^{-1}) = 6.6 \times 10^{-6} \cdot I;$$

where I (W m^{-2}) is average shortwave radiation intensity in the mixed layer.

Qureshi et al. [2010] proposed a three-species pathway for reduction and oxidation of mercury in the ocean water (see Section 2.1.1). In this model the mercury reduction rate constant at any intensity could be calculated through following equation: $k_r(I) = \alpha \times I$, where α = 0.10 – 0.15 (0.12) h^{-1} (W m^{-2})$^{-1}$.

The oxidation rate constants k_1 or k_1' increase with increasing radiation intensity for both UV-B and UV-A radiations:

$k_1(I) = \beta \times I + k_{dark}$; where β = 0.10 - 0.23(0.15) h^{-1} (W m^{-2})$^{-1}$; k_{dark}=0.31-0.8(0.5) h^{-1};

$k'_1(I) = \gamma \times I + k'_{dark}$; where γ = 0.10 - 0.23 (0.15) h^{-1}(W m^{-2})$^{-1}$; k'_{dark}=0.39-0.93 (0.6) h^{-1}.

However, the rate constants k_2 and k_2' are independent of the intensity of radiation (k_2 = 0.11-0.16 (0.13) h^{-1}; k'_2= 0.09-0.13 (0.11) h^{-1}) and have similar values for both filtered and unfiltered water samples [*Qureshi et al.*, 2010].

4.2.2. Redox processes under dark conditions

4.2.2.1. Dark reduction

The investigation of mercury reduction process in the dark, which were carried out during the cruises, showed that reduction does occur under the dark conditions in unfiltered seawater, but that the rate constants are 2–20 times slower than those in the surface waters under solar light. Since little oxidation or reduction was observed in filtered estuarine water in the dark, it was concluded that the dark reactions are microbially mediated [*Whalin et al.*, 2007]. This conclusion is confirmed by others investigators. So, *Rolfhus* and *Fitzgerald* [2004] estimated that about 20% of the photoreduction reactions in Long Island Sound were microbially mediated. Mercury biotic reduction may occur, for example, by heterotrophic bacteria [*Mason et al.*, 1995; *Siciliano et al.*, 2002; *Barkay et al*., 1989] and by algae; thus, this process can play a role for detoxification [*Ben-Bassat and Mayer,* 1977, 1978; *Whalin et al*., 2007].

Soerensen et al. [2010] assumed that biotic reduction rate constant correlate with the net primary productivity and could be described by equation $k = 4.5 \times 10^{-6} \cdot NPP$; where NPP (mg C m^{-2} d^{-1}) is net primary productivity.

A list of published reduction rate constants in seawaters under dark conditions is presented in Table 4.5. Dark reduction rate constants ranged from 2.8×10^{-8} s^{-1} to 8.3×10^{-5} s^{-1}.

Table 4.5. *Dark reduction rate constants of Mercury in seawater*

Location	Rate constants, s^{-1}	Comments	Sources
Open Atlantic Ocean (41°51′N, 60° 46′W) at a depth of 3 m below the surface	2.8×10^{-8}		*Strode et al.* [2007]
Chesapeake Bay and shelf	$(5.5 - 19.4) \times 10^{-7}$-	Isotope amended deep water (<5m from sediments)	*Whalin et al.* [2007].
(Used for model)	*min*: 3.5×10^{-7} s^{-1} *max*: 8.3×10^{-5} s^{-1}	Biotic reduction rate constant	*Soerensen et al.* [2010]

4.2.2.2. Dark oxidation

Amyot et al. [1997] have found that in the coastal waters of the Gulf of Mexico dissolved elemental mercury was oxidized under the dark conditions, and oxidation rate was estimated from 0.1 to 0.4 h^{-1}. In similar experiments with river water, these authors showed that the oxidation rates are greater in the presence of high concentrations of chloride ions. Also, rate of mercury oxidation reaction was found to depend on the presence of particles or colloids. However, results of these experiments may be insufficiently correct, because of the loss of elemental mercury from solution through volatilization of Hg(0) and/or adsorption of Hg(II) on the walls of containers used in the experiments [*Lalonde et al.,* 2001].

In more recent study, *Lalonde et al.* [2001] found that the rate of oxidation of Hg(0) in water from Baie Saint-Paul kept in the dark is significant, but about 10 times slower than that kept in the light (k =0.06 h^{-1} vs k = 0.58 h^{-1}), assuming first-order kinetics. Also, *Lalonde et al.* [2004] in investigation of waters from the St. Lawrence Estuary observed no significant loss of Hg(0) under the dark conditions. *Amyot et al*. [2005] agreed with previous authors and in their experiments found that dissolved Hg(0) did not rapidly oxidize in the presence of chloride ion or O_2 in the dark.

A list of published oxidation rate constants in seawaters under dark conditions is presented in Table 4.6. Dark oxidation rate constants ranged from $1.0x10^{-7}$ s^{-1} to 2.2×10^{-4} s^{-1}.

Table 4.6. *Dark oxidation rate constants of Mercury in seawater*

Location	Rate constants, s^{-1}	Comments	Sources
Coastal waters of the Gulf of Mexico	$(0.25 - 0.33) \times 10^{-4}$	The most likely oxidant would be O_2	*Amyot et al.* [1997]
Open Atlantic Ocean (41°51′N, 60° 46′W) at a depth of 3 m below the surface	$(0.86 - 2.22) \times 10^{-4}$	For Pathway (I)	*Qureshi et al*. [2010]
Open Atlantic Ocean (41°51′N, 60° 46′W) at a depth of 3 m below the surface	$(1.08 - 2.58) \times 10^{-4}$	For Pathway (II)	*Qureshi et al*. [2010]
St. Lawrence estuary	1.67×10^{-5}		*Lalonde et al*. [2004]
Used for modelling	1.0×10^{-7}		*Soerensen et al*. [2010]

In addition, some oxidation in the absence of light (so-called “dark” oxidation) [*Amyot et al.*, 2007; *Zhang and Lindberg*, 2001] is effected by hydroxyl radicals produced from the photochemically produced hydrogen peroxide via the Fenton reaction [*Zhang and Lindberg*, 2001]. Accordingly, the kinetics of oxidation reaction under dark conditions depend on the intensity and duration of prior light exposure [*Zhang and Lindberg,* 2001; *Lalonde et al.,* 2001; *Garcia et al.,* 2005; *Krabbenhoft et al.,* 1998*; Qureshi et al.*, 2010].

4.3. Adsorption Processes of Mercury in the Ocean

In the ocean, mercury can be involved into various biogeochemical processes, among which adsorption of bivalent mercury Hg (II) and methylmercury onto suspended particles and sediments is very important for determining the fate of mercury [*Liu et al.*, 2012]. Phase speciation and size distribution of mercury in the ocean influence it bioavailability, toxicity, and fate. For example, only the solution-phase or free ion species of mercury are bioavailable to phytoplankton [*Tessier and Turner*, 1995; *Choe et al*., 2003a].

Mercury is observed to be occurring in the ocean water in the following phases: the dissolved phase, the colloidal phase, and suspended phase. The distribution of mercury between these phases depends on the seasonal changes, location (e.g. bathymetric depth), and it is also influenced by presence of microorganisms, primarily phytoplankton and bacteria, which form so-called organic suspension [*Bonzke*, 2005].

4.3.1. Nature of particles

It was supposed that the most of particulate mercury bound to the organic suspension [*Bryan and Langston*, 1992; *Bonzke et al.*, 2005]. The strong positive correlation is observed between the concentration of total mercury and the content of organic matter in bottom sediments, which were measured in different parts of the world [*Degetto et al*., 1997; *Muhaya et al*., 1997; *Bonzke*, 2005].

Other investigators consider that both types of solid particles, inorganic minerals (e.g., metal oxides) and organic matter (e.g., humic substances), take part in the mercury adsorption process and its enrichment on solids [*Nriagu*, 1979; *Stein et al.*, 1996]. Many factors influence the relative importance of inorganic and organic matter in mercury adsorption, for example, the nature of the solid particles and mercury speciation [*Liu et al.*, 2012].

Mercury adsorption on organic matter is suggested to occur through the association of mercury with S-, O-, and N-containing functional groups within organic matter, including reduced S groups such as thiols, sulfides, and disulfides [*Liu et al.*, 2012; *Skyllberg et al.*, 2006; *Skyllberg*, 2008].

Mercury adsorption on inorganic minerals involves a formation of stable inner-sphere-type surface complexes through condensation reaction between a hydroxyl group on hydroxylated mercury species and a hydroxyl on the mineral surfaces [*Liu et al.*, 2012].

4.3.2. Rates of mercury adsorption

Mercury adsorption is usually a fast process. This conclusion was suggested by several experiments estimating rate of mercury adsorption process [*Lockwood and Chen*, 1973, *Liu et al.*, 2012].

When describing mercury adsorption, a fundamental parameter describing the distribution of a chemical species between the dissolved and solid phases in a summarizing way is a distribution (partition) coefficient (Kd, L/kg), which is often calculated [*Stumm*, 1992; *Ullrich et al*., 2001; *Liu et al.*, 2012].

The partition coefficient (K_d) for mercury is the ratio of adsorbed mercury concentration to the dissolved mercury concentration at equilibrium [*Soerensen et al.*, 2010]:

$$K_d = \frac{C_s}{C_d} \ ,$$

where C_s is the suspended particulate matter (SPM) concentration of Hg(II) on a dry weight (mass/mass) basis expressed in pg of metal per kg of sorbing material, and C_d is the filtered concentration (mass/volume) of Hg(II) in seawater expressed in pg of metal per L of solution [*Soerensen et al.*, 2010].

Despite the partition coefficient is not a true thermodynamic parameter, it has been widely used to describe the adsorption processes because of its simplicity [*Stordal et al.* 1996*a; Wen et al.* 1999; *Leermakers et al*. 2001].

Method of K_d calculating leads to negative proportionality of K_d to SPM concentration, this phenomenon was termed as the ‘‘particle concentration effect’’ [*Benoit*, 1995]. For example, experiments by *Choe et al.* [2003a] showed that in unfiltered samples the contribution of particulate mercury to the total mercury is small when the SPM concentration is low (< ~20 mg L^{-1}) and increases nonlinearly with increasing SPM concentration. When the SPM concentration is high (>30 mg L^{-1}), the Hg exists predominantly (>90%) in particulate phase [*Choe et al.*, 2003a].

Partition coefficient K_d depends on the nature of suspended solids or sediment and key geochemical parameters of the water, which primarily include the pH of the system and the nature and concentration of sorbents. Table 4.7 shows K_d values for mercury in natural environments (values shown are log K_d values).

Table 4.7. *Partition Coefficients (log K_d in L/kg) from the Literature Search*

N	logK_d	Source	Note
1	*Suspended Matter/Water* Median 5.3 (range 4.2 - 6.9) *DOC/Water* Median 5.3(range 5.3 - 5.6) *Sediment/Water* Median 4.9 (range 3.8 - 6.0)	*Allison and Allison* [2005]	from literature survey
2	5.5	*Soerensen et al.* [2010] from [*Mason and Fitzgerald,* 1993; *Mason et al*., 1998]	for marine environments
3	*In September–October 2000* 5.64 ± 0.16 *In March 2001* 5.46 ± 0.30	*Choe et al.* [2003a]	in San Francisco Bay estuary
4	6.08	*Strode et al.* [2010]	chosen for box diffusion model
5	5.04	*Mason et al.* [1998]	in the North Atlantic
6	6.0	*Mason and Fitzgerald* [1993]	in the Equatorial Pacific

4.3.3. Colloids

Colloid is the phase which defined as inorganic or organic material in the size range of ~1 nm to ~1 μm [*Liu et al.*, 2012]. Since colloidal phase in natural aquatic systems characterized by short residence time [*Baskaran et al*. 1992; *Moran and Buesseler*, 1992] and strong reactivity with trace metals including mercury [*Honeyman and Santschi*, 1989], so colloidal material have been receiving considerable attention comparatively recently [*Benoit et al*., 1994; *Dai and Martin*, 1995; *Powell et al.* 1996; *Wen et al*., 1999, *Choe*, 2003a].

The concentration of colloidal material is proportional to SPM concentration [*Choe*, 2003a]:

$$[\text{colloid}] = k\,(\text{SPM})^x$$

where k is a constant of proportionality, and x ranges between 0.5 and 1.0 [*Honeyman and Santschi* 1989; *Benoit*, 1995]. Thus, the concentration of a colloidally associated mercury increase as SPM concentration increases [*Honeyman and Santschi,* 1988; *Benoit et al.*, 1994; *Benoit*, 1995; *Sanudo-Wilhelmy et al.,* 1996; *Quemerais et al.*, 1998; *Benoit and Rozan*, 1999].

Similar to describing of mercury adsorption on particles variations of a particle–water partition coefficient K_d can be developed:

$$K_d = \frac{\left[\ \text{particulate Hg}\ (pMol\,\text{kg}^{-1})\ \right]}{\left[\ \text{filter}-\text{passing Hg}\ (pMol\,L^{-1})\ \right]}$$

$$K_p = \frac{\left[\ \text{particulate Hg}\ (pMol\,\text{kg}^{-1}\ )\right]}{\left[\ \text{dissolved Hg}\ (pMol\,L^{-1})\ \right]}$$

$$K_c = \frac{\left[\ \text{colloidal Hg}\ (pMol\,\text{kg}^{-1})\ \right]}{\left[\ \text{dissolved Hg}\ (pMol\,L^{-1})\ \right]}$$

Filter-passing fraction include dissolved and colloidal phases, consequently, K_p values would always be greater than K_d values. If K_p values are greater than K_c values then particulate matter is a more important carrier phase of mercury than colloidal matter [*Choe*, 2003a].

Colloids significantly influence mercury adsorption on large (noncolloidal) solids and on mercury transport in the ocean. Inorganic colloids in the ocean water could produce colloidal complexes with mercury species, by that decreasing mercury adsorption on large particles and enhancing mercury transport in the ocean. Adsorption of mercury on the organic colloidal matter may enhance or

decrease mercury adsorption, depending on the nature of organic matter and solids and on other geochemical factors [*Liu et al.*, 2012].

Although both truly dissolved and colloidal mercury are present in solution, the mobility, reactivity, and bioavailability of these mercury fractions may be different. Colloidal mercury can be transported in the ocean but it is poorly bioavailable [*Liu et al.*, 2012].

The effect of colloids on the distribution of mercury species between the solution and solid phases could be accounted for, when calculating partition coefficients:

$$K_d = \frac{K_p}{1 + K_{ic} M_{ic} + K_{oc} M_{oc}}$$

where K_p is the partition coefficient of mercury between the solid and truly dissolved phases, K_{ic} (or K_{oc}) is the distribution coefficient of mercury between the inorganic (or organic) colloidal and truly dissolved fractions; M_{ic} (or M_{oc}) is the concentration of inorganic (or organic) colloids [*Liu et al.*, 2012].

Thus, when studying mercury adsorption on solids in the presence of colloids, it may be necessary to differentiate mercury into particulate, colloidal and truly dissolved phases and then to calculate various distribution coefficients of mercury species between two phases [*Liu et al.*, 2012].

4.4. Mercury methylation and demethylation processes

The most toxic mercury species commonly found in the ocean waters is monomethylmercury ($CH_3Hg(II)$) which is produced by the methylation of the reactive, ionic form, primarily Hg(II) [*Morel et al.,* 1998]. Toxicity of methylmercury is provided by its readily bioaccumulation and biomagnification to significant concentrations inside living cells and tissues of aquatic organisms, therefore, $CH_3Hg(II)$ is hazardous for aquatic ecosystems and human populations. [*Lawrence and Mason*, 2001; *Lawson and Mason*, 1998; *Sunderland et al*., 2006]. A list of published methylation/demethylation rate constants in seawaters is presented in Table 4.8.

Table 4.8. *Methylation and demethylation rate constants in seawater*

Location	Rate constants, s^{-1}	Comments	Sources
Methylation			
South San Francisco Bay, California	6.4×10^{-8}	$^{203}Hg(II)$-methylation rate constant	*Marvin-DiPasquale et al* [2007]
Mediterranean Sea	$(0.35 - 7.29) \times 10^{-7}$	oxic surface seawater	*Monperrus et al*. [2007]
Chesapeake Bay and the mid-Atlantic continental margin	$(0.37 - 4.7) \times 10^{-5}$	In bottom sediments	*Hollweg* [2010]
Bay of Fundy	3.08×10^{-7}	For sediments	*Heyes et al*. [2006]
Demethylation			
South San Francisco Bay, California	3.6×10^{-6}	$Me^{203}Hg$-degradation rate constant	*Marvin-DiPasquale* [2007]
Equatorial Pacific Ocean	10^{-8}		*Mason et al.* [1993]
Chesapeake Bay	$< 10^{-7}$	Surface water	*Whalin et al*.[2007]
Bay of Fundy	6.67×10^{-5}	For sediments	*Heyes et al*. [2006]
South and equatorial Atlantic, Deep Sea	$(0.2\text{-}2.0) \times 10^{-5}$	$(CH_3)_2Hg$-degradation in the presence of light	*Mason and Sullivan* [1999]

4.4.1. Mercury methylation

Most of the $CH_3Hg(II)$ in the ocean is derived from in situ production [*Mason and Benoit*, 2003]. The most important locations of methylmercury production are estuarine and shelf sediments; deep ocean sediments and the ocean water column [*Whalin et al.*, 2007].

In the ocean many natural biotic and abiotic processes methylate Hg(II) [*Ullrich et al.*, 2001; *Boszke et al*., 2002]. Most of investigators consider that most of the methylmercury production in aquatic

environments is produced through biotic processes, and abiotic methylation is suggested to be of secondary importance [*Ullrich et al.*, 2001; *Kempter*, 2009]. The methylation process is influenced by many factors such as availability of inorganic Hg(II), activity of microorganisms, red-ox conditions, pH, temperature, salinity, organic matter content [*Ullrich et al*, 2001; *Stein et al.*, 1996; *Morel et al.,* 1998; *Boszke et al*., 2002].

A list of published methylation and demethylation rate constants in seawaters is presented in Table 3.8. Methylation rate constants ranged from 6.4×10^{-8} s^{-1} to 4.7×10^{-5} s^{-1}.

4.4.1.1. Biotic methylation

The biotic methylation of mercury occurs mainly in anaerobic conditions, e.g. in sediments, but it can also occur, although more weak, in aerobic conditions [*Matilainen and Verta*, 1995; *Regnell et al.,* 1996]. In anaerobic conditions methylcobolamine acts as a donor of methyl groups [*Hobman et al,* 2000; *Hamasaki et al.*, 1995]. For the aerobic methylation significant role is played by sulphate reducing bacteria (SRB) [*Leemakers et al.*, 1993; *Matilainen*, 1995; *Bemiot et al*., 2001], with whose involvement in the process can be described as [*Boszke et al.*, 2002]:

$$Hg^{2+} + RCH_3^- \rightarrow CH_3Hg^+ + R'.$$

In addition, some methylmercury in the ocean can be formed in aerobic conditions as a result of conversion of dimethylmercury coming from deeper layers [*Boszke et al*., 2002].

The rate of $CH_3Hg(II)$ formation may be affected by various environmental factors through influencing the supply of bioavailable Hg(II) and/or activity of methylating microbes. In particular, methylmercury formation and accumulation depends on Hg(II) concentrations, sulfide concentrations, total organic carbon, and redox potential (Eh) [*Baeyens et al.*, 1998; *Benoit et al.*, 1999, 2001c; *Compeau and Bartha*, 1984; *Mason and Lawrence*, 1999; *Stoichev et al.*, 2004; *Sunderland et al*., 2006]. In addition, the rate of methylation decreases with increasing salinity, most probably because of the inhibitory influence of chlorine-complexes [*Boszke et al*., 2002]. The concentration of methylmercury is observed to be increased in proportion to the concentration of free sulphide ions, but then the concentration of $CH_3Hg(II)$ could be decreased, most probably because of the formation of dimethylmercury [*Boszke et al*., 2002]:

$$2CH_3Hg^+ + H_2S \rightarrow (CH_3)_2Hg + HgS + 2H^+.$$

At a too high concentration of sulphide ions, the concentration of dissolved Hg(II) is too low for methylation process because of formation hardly soluble HgS which limits the availability of HgS to SRB [*Hammerschmidt & Fitzgerald*, 2006; *Kempter*, 2009].

Altogether, methylation process appears to depend largely on the initial characteristics of a specific ecosystem which limit the biotic production of methylmercury, whether this is the pool of bioavailable Hg(II) or other factors that affect microbial activity [*Sunderland et al*., 2006]. The relative rates of production of monomethyl- and dimethylmercury are influenced by the concentration of mercury and pH of the environment. Monomethylmercury is produced easier in acidic environments, at a relatively high concentration of mercury, whereas dimethylmercury in neutral or alkaline conditions, at a relatively low concentration of mercury and in the presence of relatively strong complexing reagents such as H_2S [*Ullrich et al.,* 2001; *Galvin et al.*, 1996]. It was estimated that the rate of monomethylmercury formation is about 6000 times higher than that of dimethylmercury formation, thus, only 3% of organic mercury in the natural environment occurs as dimethyl species [*Bryan and Langston*, 1992]. The production of dimethylmercury by microorganisms and its liberation to the environment is assumed to be a detoxication mechanism [*Hobman et al*., 2000; *Leemakers et al*., 1993; *Boszke et al.,* 2002].

Methylation in oxic surface seawater

Although it is observed that the most suitable conditions for occurring of methylation process are in sediments zone, *Monperrus et al*. [2007] showed that methylmercury formation may occur in oxic surface seawater by heterotrophic organisms, mainly by phyto- and bacterioplankton. In surface coastal regions methylation rates range from 0.008 to 0.063% per d^{-1}, for open seawater methylation rates range from 0 to 0.005 d^{-1} [*Monperrus et al.*, 2007; *Kempter,* 2009]. Mercury methylation varies seasonally: high methylation rates are observed when water temperatures are high and sufficient amount of nanoplankton presents [*Monperrus et al.*, 2007].

In coastal surface water, high net methylation rates can occur during periods of high primary production and biological turnover; and methylation rates increase when metabolistic activities of phytoplankton (autotrophic) and pelagic bacteria (heterotrophic) are high. Therefore, mercury methylation is primarily biotic process [*Monperrus et al.*, 2007].

In the open ocean, highest methylation rates were observed under dark conditions for samples with high nanoplanktonic activities. Nanoplankton, which consists predominantly of autotrophic organisms, is located in the deeper euphotic zone, where only 1 to 0.1% of photosynthetic active radiation is present [*Monperrus et al.*, 2007].

4.4.1.2. Abiotic Methylation

In the marine environments, abiotic mercury methylation is regarded to be of minor importance, nevertheless it can occur [*Fitzgerald et al.*, 2007; *Kempter*, 2009].

One of the most substantial abiotic sources of methylmercury to the open ocean is an activity of hydrothermal vents and submarine volcanoes [*Kempter*, 2009]. Information of methylmercury concentrations in the deep ocean suggest that methylmercury, which is produced by hydrothermal fluids, may be apparently deposited in sediments or decomposed than transported to the surface ocean [*Lamborg et al.*, 2006; *Kempter*, 2009].

The abiotic processes of methylation can be involving irradation and without irradiation [*Hamasaki et al*., 1995]. In reactions involving irradiation the donors of methyl groups can be acetic acid, propionic acid, methanol and ethanol, while the reactions without irradiation include those with methylcobalamine, trasmethylation (methylated tin compounds) and those with humic substances [*Hamasaki et al*., 1995]. Methylated tin and lead compounds can also be potential reagents in abiotic methylation of mercury, especially in tin and lead-polluted regions [*Weber*, 1993; *Ceratti et al*., 1992; *Ebinghaus et al*., 1994]. It is suggested that humic substances are most important methylating agents for mercury because of its relatively high concentration in water environment and co-migration with mercury in water [*Weber*, 1993; *Boszke*, 2002].

4.4.2. Demethylation

Methylmecrury is relatively stable and water-soluble in deeper ocean waters and may therefore be transported long distances from its site of methylation to its site of bioaccumulation [*Mason and Fitzgerald*, 1993; *Mason et al*., 1999, 2001; *Whalin*, 2007]. However, in surface waters, methylmercury is relatively unstable to degradation. Demethylation may occur also in the water column and in sediments, and it is very important process because it results in decrease of toxic methylmercury [*Kempter*, 2009].

Experiments by *Whalin et al*. [2007] of methylmercury degradation in seawater demonstrated that the rate of this process to be within the analytical variability (<10% loss) during an incubation of several

days, or degradation rates of $<10^{-7}$ s^{-1}; much less than that for freshwater. However, experiments by *Chen et al*. [2003] showed that rates of demethylation were similar in the presence or absence of Cl^- in experiments at high concentrations (3×10^{-5} M methylmercury) under artificial light conditions. Accordingly, it is not clearly understood whether Cl^- enhances or hinders demethylation process, and other degradation pathways, such as degradation in the presence of hydroxyl radicals [*Chen et al*., 2003].

Demethylation process readily occurs in the sediments, and rate constants for demethylation are estimated to be higher than those for methylation [*Heyes et al*., 2004; 2006; *Sunderland et al.*, 2004; *Kim et al*., 2006, *Whalin et al*., 2007]. The range for demethylation rates in aquatic systems is relatively wide. A list of published methylation and demethylation rate constants in seawaters is presented in Table 3.8. Demethylation rate constants ranged from 1.0×10^{-8} s^{-1} to 2.0×10^{-5} s^{-1}.

Demethylation of mercury as well as mercury methylation can be mediated by a biological route (through microorganisms) and a abiotic route [*Hobman et al.*, 2000; *Boszke*, 2002].

4.4.2.1. Biotic demethylation

Biotic demethylation of mercury is a slow process, and as against to methylation process it is most effective in aerobic conditions [*Boszke*, 2002]. *Matilainen and Verta* [1995] demonstrated that demethylation occurs with the involvement of microorganisms, because of a great influence of decreasing temperature on the rate of demethylation and cessation of demethylation in sterilised samples of water. For demethylation process it may be demanded to occur hydrolysis of mercury-carbon bond accompanying the formation of Hg^{2+} and methane. Then Hg^{2+} may be reduced to volatile elementary mercury and released to the atmosphere where it undergoes further conversions [*Stein et al*., 1996]:

$$CH_3Hg^+ \rightarrow CH_3 + Hg^{2+};$$

$$Hg^{2+} \rightarrow Hg^{\circ}.$$

In sediments, there are two predominant pathways for demethylation: reduction and oxidation. The reduction mechanism is regarded to be carried out by bacteria which exhibit the so-called mer-operon, a genetic resistance to mercury, and represents a detoxification process. The oxidation mechanism is occurred through a C1 (one carbon) metabolism of bacteria. It must be noted that in sediments the reductive demethylation process is supposed to be the predominant [*DiPasquale et al.*, 2000].

4.4.2.2. Abiotic demethylation

Abiotic demethylation is suggested to be predominantly a photochemical process. For example, *Monperrus et al.* [2007] suggested that demethylation in coastal and marine surface waters is mainly photochemically driven. Photochemical demethylation has been shown to occur in freshwater systems and in marine waters [*Sellers et al.*, 1996; *Whalin et al*., 2007]. *Whalin et al.* [2007] found that demethylation rates for high-light conditions are increased compared to low-light conditions. Since demethylation did also occur in samples which where incubated under dark conditions, demethylation in the oceanic water column most probably does have abiotic as well as biotic components.

Dimethylmercury $(CH_3)_2Hg$ is relatively rapidly degraded in the presence of light [0.2 - 2 × 10^{-5} s^{-1}; *Mason and Sullivan*, 1999; *Whalin et al*., 2007] Dimethylmercury can be decompose to methane and elemental mercury by photolysis or oxidised by hydroxyl radical [*Stein et al.*, 1996]:

$$(CH_3)_2Hg \rightarrow Hg(0) + 2CH_3;$$

$$(CH_3)_2Hg + OH\cdot \rightarrow CH_3HgOH + CH_3.$$

In the ocean, degradation of dimethylmercury to monomethylmercury is found to be primarily an abiotic process, and its rate increases in the presence of light [*Mason,* 1991; *Mason and Sullivan,* 1999].

The results reported by *Whalin et al*. [2007] and earlier studies confirm that demethylation rates are slower in saline waters. The absence of a large difference between samples incubated in the light and dark suggests that in saline waters the process is not strongly mediated by sunlight.

The results presented by *Whalin et al.* [2007] and *Mason* [1991; 2001] suggested that methylmercury is relatively stable in ocean waters. The stability of methylmercury in seawaters is a very important parameter for estimating of quantity of methylmercury released from sediments which could be transported to the water column and then transported offshore to regions where it may be accumulated into the food chain. If the stability is as high as demonstrated by *Whalin et al.* [2007], this suggests that coastal waters may be an important source of methylmercury to open ocean waters and food chain.

5. Future activities

At MSC-W the nesting described in this report will be repeated, and expanded as we will get an updated set of emissions at a later stage. The work presented here is still an important step forward, and with the methodology presented here we have a tool to assess the effects of present and future emissions on European pollution levels in more detail than what can be achieved by global model(s) alone. Furthermore the nesting can be repeated, testing the effects of emission changes in other parts of the globe. With an updated set of emissions the modelling system will to some extent be a “plug and run” exercise.

MSC-E will continue the work on development and application of the GLEMOS multi-scale modeling system. In particular, future activities will include improvement of the modular architecture and further testing of the nesting procedure as well as enhancement of the framework computational efficiency. We also plan to incorporate aerosols and atmospheric reactants based on external datasets or simplified chemical modules for improving evaluation of HM and POP pollution levels. The comprehensive analysis of major physical and chemical processes governing mercury cycling in the atmosphere will be continued based on a sensitivity study and evaluation against detailed measurements (in co-operation with EU GMOS project).

In addition, MSC-E and MSC-W will continue co-operation with the EMEP Task Force on Hemispheric Transport of Air Pollution (TF HTAP) to develop a fuller scientific understanding of the intercontinental transport of pollutants; its impacts on health, ecosystems, and climate. In particular, the Centres will participate in a new round of the multi-model experiments including assessment of regional boundary conditions, source attribution, and sensitivities to future abetment scenarios.

REFERENCES

Allard B. and I. Arsenie [1991] Abiotic reduction of mercury by humic substances in aquatic system - an important process for the mercury cycle. *Water Air Soil Poll.,* vol. 56, pp. 457–464.

Allison J.D. and T.L. Allison [2005] Partition coefficients for metals in surface water, soil, and waste. *U.S. Environmental Protection Agency, Washington, DC*.

Amyot M., F.M.M. Morel, P.A. Ariya [2005] Dark Oxidation of Dissolved and Liquid Elemental Mercury in Aquatic Environments. *Environmental Science and Technology,* vol.39, pp.110-114.

Amyot M., G. Southworth, S.E. Lindberg, H. Hintelmann, J.D. Lalonde, N. Ogrinc, A.J. Poulain, K.A. Sandilands [2004] Formation and evasion of dissolved gaseous mercury in large enclosures amended with 200HgCl2. *Atmos. Environ.,* vol. 38, pp. 4729–4289.

Amyot M., D.R.D. Lean, L. Poissant, M.-R. Doyon [2000] Distribution and transformation of elemental mercury in the St. Lawrence River and Lake Ontario. Can. *J. Fish. Aquat. Sci*., vol. 57 (supplement 1), pp.155–163.

Amyot M., G.A. Gill and F.M.M. Morel [1997]. Production and loss of dissolved gaseous mercury in coastal seawater. *Environmental Science and Technology,* vol. 31, pp. 3606-3611.

Amyot M., G. Mierle, D.R.S. Lean, D.J. McQueen [1994] Sunlight induced formation of dissolved gaseous mercury in lake waters. *Environ. Sci. Technol.*, vol. 28, pp.2366–2371.

Baeyens W., C. Meuleman, M. Leermakers [1998] Behavior and speciation of mercury in the Scheldt estuary (water, sediment and benthic organisms). *Hydrobiologia*, vol. 366, pp.63–79.

Barkay T., C. Liebert, M. Gillman [1989] Environmental significance of the potential for mer(Tn21)-mediated reduction of Hg2+ to Hg0 in natural waters. *Appl. Environ. Microbiol*., vol. 55, pp. 1196–1202.

Bash J.O. and E.J. Cooter [2008] Bi-directional mercury exchange over surface waters simulated by a regional air pollution model(poster presentation). 88th American Meteorological Society Annual Meeting, New Orleans, LA, 20-24 January, 2008.

Baskaran M., P. H. Santschi, G. Benoit, And B. D. Honeyman [1992] Scavenging of thorium isotopes by colloids in seawater of the Gulf of Mexico. *Geochim. Cosmochim. Acta*., vol. 56**,** pp. 3375– 3388.

Ben-Bassat D. and A.M. Mayer [1977] Reduction of mercury chloride by Chlorella: evidence for a reducing factor. *Physiol. Plant*. vol. 40, pp. 157–162.

Ben-Bassat D. and A.M. Mayer [1978] Light-induced volatilization and O2 evolution in Chlorella and the effect of DCMU and methylamine. *Physiol. Plant*., vol. 42, pp.33–38.

Benoit J.M., C.C. Gilmour and R.P. Mason [2001a] Aspects of bioavailability of mercury for methylation in pure cultures of *Desulfobulbus propionicus* (1pr3). *Applied and Environmental Microbiology,*vol. 67 (1), pp. 51-58.

Benoit J.M., C.C. Gilmour and R.P. Mason [2001b] The influence of sulfide on solid-phase mercury bioavailability for methylation by pure cultures of Desulfobulbus propionicus (1pr3). *Environmental Science and Technology,* vol. 35, pp.127–132.

Benoit J.M., R.P. Mason, C.C. Gilmour and G.R. Aiken [2001c] Constants for Mercury Binding By Dissolved Organic Matter Isolates from the Florida Everglades. *Geochemica et Cosmochimica Acta*., vol. 65 (24), pp. 4445-4451.

Benoit J., C.C. Gilmour, R.P. Mason, A. Heyes [1999] Sulfide controls on mercury speciation and bioavailability to methylating bacteria in sediment pore waters. *Environmental Science and Technology,* vol. 33, pp. 951–957.

Benoit J.M. and T.F. Rozan [1999] The influence of size distribution on the particle concentration effect and trace metal partitioning in rivers. *Geochim. Cosmochim. Acta,* vol. 63**,** pp. 112–127.

Benoit J. [1995] Evidence of the particle concentration effect for lead and other metals in fresh waters based on ultraclean technique analyses. *Geochim. Cosmochim. Acta*, vol. 59, pp. 2677–2687.

Benoit J., S. D. Oktay-Marshall, A. Cantu Ii, E. M. Hood, C. H. Coleman, M. O. Corapcioglu, and P. H. Santschi [1994] Partitioning of Cu, Pb, Ag, Zn, Fe, Al, and Mn between filterretained particles, colloids, and solution in six Texas estuaries. *Mar. Chem*. 45: 307–336.

Bloom N.S. [1992] On the chemical form of mercury in edible fish and marine invertebrate tissue. *Canadian Journal of Fisheries and Aquatic Sciences,* vol. 49, pp. 1010-1017.

Bonzongo and Donkor [2003] Increasing UV-B radiation at the earths surface and potential effects on aqueous mercury cycling and toxicity

Boszke L., G. Głosińska, J Siepak [2002] Some Aspects of Speciation of Mercury in a Water Environment. Polish *Journal of Environmental Studies* , vol. 11, Issue: 4, pp. 285-298 ISSN: 12301485.

Bryan G.W. and W.J. Langston [1992] Bioavailability, accumulation and effects of heavy metals with special reference to United Kingdom estuaries: a review. *Environ. Pollut.*, vol.76, p. 89.

Ceratti G., M. Bernhard, J.H. Weber [1992] Model reactions for abiotic mercury (II) methylation: kinetics of methylation of mercury (II) by mono-, di- and tri- methyltin in seawater. *Applied Organomet. Chem.*, vol. 6, p. 587.

Chen J., S.O. Pehkonen, C.-J. Lin [2003] Degradation of monomethylmercury chloride by hydroxyl radicals in simulated natural waters. *Water Res.*, vol. 37, pp.2496–2504.

Choe K.-Y., G.A. Gill and R.D. Lehman [2003a] Distributions of particulate, colloidal and dissolved mercury in the San Francisco Bay estuary: 1. Total mercury. *Limnology and Oceanography*, vol. 48 (4), pp. 1535-1546.

Choe K.-Y. and G.A. Gill [2003b] Distributions of particulate, colloidal and dissolved mercury in the San Francisco Bay estuary: 2. Monomethyl mercury. *Limnology and Oceanography*, vol. 48 (4), pp. 1547-1556.

Compeau G. and R. Bartha [1984] Methylation and demethylation of mercury under controlled redox, pH, and salinity conditions. *Applied and Environmental Microbiology*, vol. 48, pp. 1203– 1207.

Cossa D., J. M. Martin, K. Takayanagi, and J. Sanjuan [1997] The distribution and cycling of mercury species in the western Mediterranean, *Deep Sea Res*., Part II, 44(3–4), 721–740.

Cossa D., M.H. Cotte-Krief, R.P. Mason and J. Bretaudeau-Sanjuan [2004] Total mercury in the water column near the shelf edge of the European continental margin, *Mar. Chem*., 90, 21– 29.

Costa M. and P.S. Liss [1999] Photoreduction of mercury in sea water and its possible implications for elemental Hg air–sea fluxes. *Mar. Chem*., vol. 68, pp.87–95.

Dai M. and Martin J.-M. [1995] First data on trace metal level and behaviour in two major Arctic river-estuarine systems (Ob and Yenisey) and in the adjacent Kara Sea, Russia. *Earth Planet. Sci. Lett.* vol.131, pp. 127–141.

Dalziel J.A. [1995] Reactive mercury in the eastern North Atlantic and southeast Atlantic. *Mar. Chem.*, vol. 49, pp. 307– 314.

Degetto S., M. Schintu, A. Contu, G. Sbrignadello [1997] Santa Gilla Lagoon (Italy): a mercury sediment pollution case study. Contamination assessment and restoration of the site. *Sci. Total Environ*., vol. 204, p. 49.

DiPasquale M.M., J. Agee, C. McGowan, R.S. Oremland, M. Thomas, D. Krabbenhoft, C.C. Gilmour [2000] Methylmercury degradation pathways: A comparison among three mercury-impacted ecosystems. *Environmental Science & Technology,* vol. 34(23), pp. 4908–4916.

EMEP Transboundary acidification, eutrophication and ground levelozone in Europe in 2010. Joint MSC-W & CCC & CEIP Report. EMEP Status Report 1/2012.

Ebinghaus R., H. Hintelman, R.D. Wilken [1994] Mercury-cycling in surface waters and in the atmosphere - species analysis for the investigation of transformation and transport properties of mercury. *Fresenius J. Anal. Chem*., vol. 350**,** p. 21.

Fitzgerald W.F., C.H. Lamborg, D.H. Heinrich, K.T. Karl [2007] Geochemistry of mercury in the environment, treatise on geochemistry. *Oxford: Pergamon*, pp.1-47.

Galvin R.M. [1996] Occurrence of metals in waters: an overview. *Water S.A*., vol. 22**,** p. 7.

Garcia E., A.J. Poulain, M. Amyot, P. Ariya [2005] Diel variations in photoinduced oxidation of Hg0 in freshwater. *Chemosphere,* vol. 59, pp. 977–981.

Gårdfeldt K. and M. Jonsson [2003] Is bimolecular reduction of Hg(II) complexes possible in aqueous systems of environmental importance. *J. Phys. Chem. Atm.*, vol. 107, pp. 4478–4482.

Gårdfeldt K., J. Sommar, D. Stromberg, X. Feng [2001] Oxidation of atomic mercury by hydroxyl radicals and photoinduced decomposition of methyl mercury in the aqueous phase. *Atmos. Environ.*, vol. 35, pp. 3039–3047.

Gill G.A. [2008] Transport, Cycling, and Fate of Mercury and Monomethyl Mercury in the San Francisco Delta and Tributaries: An Integrated Mass Balance Assessment Approach (Task 5.4 Air-Water Exchange Studies) *Final Report Submitted to the Calfed Bay-Delta Program as Part of the Calfed Mercury Project Entitled: Assessment of Ecological and Human Health Impacts of Mercury in the Bay-Delta Watershed* http://mercury.mlml.calstate.edu/reports/reports/

Gill G.A. and W. F. Fitzgerald [1988] Vertical mercury distributions in the oceans, *Geochim. Cosmochim. Acta*, vol. 52, pp. 1719– 1728.

Gusev A., O. Rozovskaya, V. Shatalov, V.Sokovykh [2009] Persistent Organic Pollutants in the Environment. EMEP Status Report 3/2009.

Gusev A., S.Dutchak, O.Rozovskaya, V.Shatalov, V.Sokovykh, N.Vulykh [2011] Persistent Organic Pollutants in the Environment. EMEP Status Report 3/2011.

Hamasaki T., H. Nagase, Y. Yoshioka, T. Sato [1995] Formation, distribution, and ecotoxicology of methylmetals of tin, mercury, and arsenic in the environment. Critical Review in *Environ. Sci. Technol*., vol. 25, p. 45.

Hammerschmidt C.R. and W.F. Fitzgerald [2006]. Methylmercury cycling in sediments on the continental shelf of southern New England. *Geochemica et Cosmochimica Acta,* vol. 70(4), pp. 918–930.

Heyes A., C. Miller, R.P. Mason [2004] Mercury and methylmercury in Hudson River sediment: impact of tidal resuspension on partitioning and methylation. *Mar. Chem*., vol. 90, pp. 75–89.

Heyes A., R.P. Mason, E. Kim, E. Sunderland [2006] Mercury methylation in estuaries: insights from using measuring rates using stable mercury isotopes. *Mar. Chem*., vol. 102, pp. 134–147.

Hines N.A., and P.L. Brezonik [2004]. Mercury dynamics in a small Northern Minnesota lake: water to air exchange and photoreactions of mercury. *Marine Chemistry,* vol. 90, pp. 137-149.

Hobman J.L., J.R. Wilson, N.L. Brown [2000] Microbial Mercury Reduction. In: Environmental Microbe-Metal Interaction. *Lovley D. R. (ed.) ASM Press, Washington.*

Hollweg T.A. [2010] Mercury cycling in sediments of Chesapeake Bay and the Mid-Atlantic continental shelf and slope. *Ph.D. thesis. University of Connecticut*.

Honeyman B.D. and P.H. Santschi [1989] A brownian-pumping model for oceanic trace metal scavenging: Evidence from thorium isotopes. *J. Mar. Res.,* vol. 47**,** pp. 951–992.

Honeyman B.D.,and P.H. Santschi [1988] Metals in aquatic systems. *Environ. Sci. Technol.,* vol. 22, pp. 862–871.

HTAP: HTAP 2010 Assessment Report. GenevaØ UN-Economic Commission for Europe (Available at URL: www.htap.org), 2010.

Jonson, J.E, A. Stohl, A. M. Fiore, P. Hess, S. Szopa, O. Wild, G. Zeng, F. J. Dentener, A. Lupu, M. G. Schultz, B. N. Duncan, K. Sudo, P. Wind, M. Schulz, E. Marmer, C. Cuvelier, T. Keating, A. Zuber, A. Valdebenito, V. Dorokhov, H. De Backer, J. Davies, G. H. Chen, B. Johnson, D. W. Tarasick, R. Stübi, M.J. Newchurch, P. von der Gathen, W. Steinbrecht, and H. Claude: A multi-model analysis of vertical ozone profiles. Atmos. Chem. Phys.., 10, 5759-5783, 2010.

Kallenborn R., Christensen G., Evenset A., Schlabach M, Stohl A. [2007] Atmospheric transport of persistent organic pollutants (POPs) to Bjornova (Bear Island). *J. Environ. Monit*. Oct; vol. 9(10), pp. 1082-91.

Kempter T. [2009] Cycling of monomethylmercury in the ocean, an exploration of sources and sinks. *ETHZ - Term Paper in Biogeochemistry and Pollutant Dynamics,* pp. 1-17.

Kim E-H., R.P. Mason, E.T. Porter, H.L. Soulen [2006] The effect of sediment resuspension on the fate and bioaccumulation of mercury in estuarine sediments. *Mar. Chem*., vol. 102, pp. 300–315.

Krabbenhoft D.P., J.P. Hurler, M.L. Olson, L.B. Cleckner [1998] Diel variability of mercury phase and species distributions in the Florida Everglades. *Biogeochemistry,* vol. 40, pp. 311–325.

Lalonde J.D., M. Amyot, J. Orvoine, F.M.M. Morel, J.-C. Auclair, P.A. Ariya [2004]. Photoinduced oxidation of Hg0(aq) in the waters from the St. Lawrence Estuary. *Environ. Sci. Technol.*, vol. 38, pp. 508–514.

Lalonde J.D., M. Amyot, A.M.L. Kraepiel, F.M.M. Morel [2001] Photooxidation of Hg(0) in artificial and natural waters. *Environ. Sci. Technol*., vol. 35, pp. 1367–1372.

Lamborg C.H., K.L. Damm. W.F. Von Fitzgerald, C.R. Hammerschmidt, R. Zierenberg [2006] Mercury and monomethylmercury in fluids from Sea Cliff submarine hydrothermal field, Gorda Ridge. *Geophysical Research Letters*, vol. 33(17).

Lamborg C.H., C-M. Tseng, W. F. Fitzgerald, P.H. Balcom and C.R. Hammerschmidt [2002]. Determination of the Mercury Complexation Characteristics of Dissolved Organic Matter in Natural Waters with "Reducible Hg" Titrations. *Environmental Science and Technology*., vol 37 (15), pp. 3316-3322.

Laurier F.J.G., R.P. Mason, G.A. Gill and L. Whalin [2004] Mercury distributions in the North Pacific Ocean: 20 years of observations, *Mar. Chem.*, vol. 90, pp. 3– 19.

Lawrence A.L. and R.P. Mason [2001] Factors controlling the bioaccumulationof mercury and methylmercury by the estuarine amphipod Leptocheirus plumulosus. *Environmental Pollution*, vol. 111, pp. 217–231.

Lawson N.M. and R.P. Mason [1998] Accumulation of mercury in estuarine food chains. *Biogeochemistry*, vol. 40, pp. 235– 247.

Leermakers, M., S. Galletti, S. De Galan, N. Brion and W. Baeyens [2001] Mercury in the southern North Sea and Scheldt estuary. *Mar. Chem*., vol. 75, pp. 229–248.

Lepane V., T. Persson, M. Wedborg [2003] Effects of UV-B radiation on molecular weight distribution and fluorescence from humic substances in riverine and low salinity water. *Estuar. Coast. Shelf. S.,* vol. 56, pp. 161–173.

Lin C.-C., N. Yee, T. Barkay [2012] Microbial transformations in the mercury cycle, in *Environmental Chemistry and Toxicology of Mercury*, First Edition, edited by G. Liu, Y. Cai, N. O'Driscoll, *John Wiley & Sons, Inc.*, pp.155-192.

Lin C.-J. and S.O. Pehkonen [1999] Aqueous phase reaction of mercury with free radicals and chlorine: implications for atmospheric mercury chemistry. *Chemosphere*, vol. 38, pp. 1253–1263.

Liu G., Y. Li, Y. Cai [2012] Adsorption of mercury on solids in the aquatic environment, in *Environmental Chemistry and Toxicology of Mercury*, First Edition, edited by G. Liu, Y. Cai, N. O'Driscoll, *John Wiley & Sons, Inc.*, pp.367-387

Liu H., X.Z. Li, Y.J. Leng, C. Wang [2007] Kinetic modeling of electro-Fenton reaction in aqueous solution. *Water Res.* , vol. 41, pp. 1161–1167.

Lockwood R.A. and K.Y. Chen [1973] Adsorption of mercury(II) by hydrous manganese oxides. *Environmental science and technologies*, vol. 7, pp. 1028-1034.

Luther III G.W. and E. Tsamakis [1989] Concentration and form of dissolved sulfide in the oxic water column of the ocean. *Mar. Chem.,* vol. 127, pp. 165–177.

Mason R.P. and G.A. Gill [2005] Mercury in the marine environment, in Mercury: Sources, Measurements, Cycles and Effects, edited by M. B. Parsons and J. B. Percival, pp. 179 – 216, *Short Course Ser.*, vol. 34, Mineral. Assoc. of Canada, Halifax, Nova Scotia, Canada.

Mason R.P. and J.M. Benoit [2003] Organomercury compounds in the environment. In: Craig, P. (Ed.), Organometallics in the Environment. John Wiley & Sons, New York, pp. 57–99.

Mason R.P. and G.R. Sheu [2002] Role of the ocean in the global mercury cycle, *Global Biogeochem. Cycles,* vol. 16(4), p. 1093, doi:10.1029/ 2001GB001440.

Mason R.P., N.M. Lawson, G.-R. Sheu [2001] Mercury in the Atlantic Ocean: factors controlling air–sea exchange of mercury and its distribution in the upper waters. Deep-Sea Res., Part 2, *Top. Stud. Oceanogr*., vol. 48, pp. 2829–2853.

Mason R.P. and K.A. Sullivan [1999] The distribution and speciation of mercury in the south and equatorial Atlantic, Deep Sea Res., Part II, vol. 46, pp. 937– 956.

Mason R.P. and A.L. Lawrence [1999] Concentration, distribution, and bioavailability of mercury and methylmercury in sediments of Baltimore Harbor and Chesapeake Bay, Maryland, USA. *Environmental Toxicology and Chemistry*, vol. 18, pp. 2438– 2447.

Mason R.P., K.R. Rolfhus and W.F. Fitzgerald [1998] Mercury in the North Atlantic. *Mar. Chem.*, vol. 61, pp. 37–53.

Mason R.P. and W.F. Fitzgerald [1996] Sources, sinks and biogeochemical cycling of mercury in the ocean. In: Baeyens, W., et al. (Ed.), Global and Regional Mercury Cycles: Sources, Fluxes and Mass Balances. Kluwer Academic, Netherlands, pp. 249–272.

Mason R.P., F.M.M. Morel, H.F. Hemond [1995] The role of microorganisms in elemental mercury formation in natural waters. *Water Air Soil Poll.*, vol. 80, pp. 775–787.

Mason R.P., W.F. Fitzgerald, F.M.M. Morel [1994] The biogeochemical cycling of elemental mercury: Anthropogenic influences. *Geochim. Chosmochim. Acta*., vol. 58, pp. 3191-3198.

Mason R.P. and Fitzgerald [1993] The distribution and cycling of mercury in the equatorial Pacific Ocean. *Deep-Sea Research Part 1: Oceanographic Research Papers, Deep Sea Res.,* vol. 40, pp. 1897– 1924.

Mason R.P., Fitzgerald W.F., Hurley J.P., Hanson Jr., J.K., Donaghay P.L., Sieburth J.M. [1993] Mercury biogeochemical cycling in a stratified estuary. *Limnol. Oceanogr.* vol. 38, pp. 1227–1241.

Mason R.P. [1991] The chemistry of mercury in the equatorial Pacific Ocean. PhD dissertation, University of Connecticut, Storrs, CT.

Mason R.P. and W.F. Fitzgerald [1991] Mercury speciation in open ocean waters. *Water Air Soil Pollut*., vol. 56, pp. 779– 789.

Matilainen T. [1995] Involvent of bacteria in methylmercury formation in anaerobic lake waters. *Water, Air & Soil Pollut.*, vol. 80, p. 757.

Matilainen T. and M. Verta [1995] Mercury methylation and demethylation in aerobic surface waters. *Can. J. Fish. Aquat. Sci.* vol. 52, p. 1597.

Monperrus M., E. Tessier, D. Amouroux, A. Leynaert, P. Huonnic, O.F.X. Donard [2007] Mercury methylation, demethylation and reduction rates in coastal and marine surface waters of the Mediterranean Sea. *Marine Chemistry*, vol. 107(1), pp. 49–63.

Mopper K. and X. Zhou [1990] Hydroxyl radical photoproduction in the sea and its potential impact on marine processes. *Science,* vol. 250, pp. 661–664.

Moran S.B. and K.O. Buesseler [1992] Short residence time of colloids in the upper ocean estimated from ^{238}U-^{234}Th disequilibria. *Nature*, vol. 359, pp. 221–223.

Morel F.M.M., A.M.L. Kraepiel and M. Amyot [1998] The chemical cycle and bioaccumulation of mercury. *Annual Review Ecology and Systematics*, vol. 29, pp. 543-566.

Morel F.M.M. and J.G. Hering [1993] Principles and Applications of Aquatic Chemistry. *New York, NY, John Wiley & Sons, Inc.*

Muhaya B.B.M., M. Leermakers, W. Baeyens [1997] Total mercury and methylmercury in sediments and in the polychaete *Nereis diversicolor* at Groot Buitenschoor (Sheldt Estuary, Belgium). *Water, Air & Soil Pollut.*, vol. 94, p. 109.

Nriagu J. [1979] The biogeochemistry of mercury in the environment. *New York (NY): Elsevier/North Holland Biomedical Press*; p. 696

O'Driscoll N.J., S.D. Siciliano, D.R.S. Lean, M. Amyot [2006] Gross photoreduction kinetics of mercury in temperate freshwater lakes and rivers: application to a general model of DGM dynamics. *Environ. Sci. Technol.*

O'Driscoll N.J., A.N. Rencz, D.R.S. Lean [2005] Chapter 14: The biogeochemistry and fate of mercury in natural environments. In: *Metal Ions in Biological Systems*; Sigel, A., Sigel, H., Sigel, R. K. O., Eds.; Marcel Dekker: New York, vol 43.

O'Driscoll N.J., S. Beauchamp, S.D. Siciliano, A.N. Rencz and D.R.S. Lean [2003a]. Continuous analysis of dissolved gaseous mercury (DGM) and mercury flux in two freshwater lakes in Kejimkujik Park, Nova Scotia: evaluating mercury flux models with quantitative data. *Environmental Science and Technology,* vol. 37, pp. 2226-2235.

O'Driscoll N.J., S.D. Siciliano and D.R.S. Lean [2003b]. Continuous analysis of dissolved gaseous mercury in freshwater lakes. *The Science of the Total Environment.,* vol. 304, pp. 285-294.

Ogawa H. and E. Tanoue [2003] Dissolved organic matter in oceanic waters. *J. Oceanogr.*, vol. 59, pp. 129–147.

Pirrone N, Cinnirella S, Feng X, Finkelman RB, Friedli HR, Leaner J, Mason R, Mukherjee AB, Stracher G, Streets DG, Telmer K [2009] Global mercury emissions to the atmosphere from natural and anthropogenic sources, in *Mercury Fate and Transport in the Global Atmosphere: Emissions, Measurements, and Models*, edited by N. Pirrone and R. P. Mason, Springer, pp. 3-49

Poissant L, A. Dommergue and C.P. Fefferi [2002] Mercury as a global pollutant. *J. Phys. IV France*, vol. 12, DOI: 10.1 051/jp4:2 0020457

Powell R. T., W. M. Landing, And J. E. Bauer [1996] Colloidal trace metals, organic carbon and nitrogen in a southeastern U.S. estuary. *Mar. Chem.,* vol. 55, pp. 165–176.

Quemerais B., D. Cossa, B. Rondeau, T. T. Pham, And B. Fortin [1998] Mercury distribution in relation to iron and manganese in the waters of the St. Lawrence River. *Sci. Total Environ.,* vol. 213, pp. 193–201.

Qureshi A., N.J. O'Driscoll, M. MacLeod, Y.M. Neuhold, K. Hungerbuhler [2010] Photoreactions of mercury in surface ocean water: gross reaction kinetics and possible pathways. *Environ. Sci. Technol.*, vol. 44 (2), pp. 644–649.

Regnell O., A. Tunlid, G. Ewald, O. Sangfors [1996] Methyl mercury production in freshwater microcosms affected by dissolved oxygen levels: role of cobolamin and microbial community composition. *Can. J. Fish. Aquat. Sci*., vol. 53, p. 1535.

Rolfhus K.R. and W.F. Fitzgerald [2004] Mechanisms and temporal variability of dissolved gaseous mercury production in coastal seawater. *Mar. Chem*., vol. 90, pp. 125–136.

Sanudo-Wilhelmy S. A., I. Rivera-Duarte, And A. R. Flegal [1996] Distribution of colloidal trace metals in the San Francisco Bay estuary. *Geochim. Cosmochim. Acta,* vol. 60, pp. 4933–4944.

Sellers P., C.A. Kelly, J.W.M. Rudd, A.R. MacHutchon [1996]. Photodegradation of methylmercury in lakes. *Nature*, vol. 380, pp.694–697.

Shatalov V., A. Gusev, S. Dutchak, O. Rozovskaya, V. Sokovykh, N. Vulykh [2010] Persistent Organic Pollutants in the Environment. EMEP Status Report 3/2010.

Siciliano S. D., N.J. O'Driscoll, D.R.S Lean [2002] Microbial reduction and oxidation of mercury in freshwater lakes. *Environ. Sci. Technol.*, vol. 36, pp. 3064–3068.

Skyllberg U. [2008] Competition among thiols and inorganic sulfides and polysulfides for Hg and MeHg in wetland soils and sediments under suboxic conditions: illumination of controversies and implications for MeHg net production. *J.Geophys Res*, 113: G00C03. DOI: 10.1029/2008JG000745.

Skyllberg U., Bloom P.R., Qian J., Lin C.M., Bleam W.F. [2006] Complexation of mercury(II) in soil organic matter: EXAFS evidence for linear two-coordination with reduced sulfur groups. *Environ Sci Technol.*, vol. 40, pp. 4174-4180

Soerensen A.L., E.M. Sunderland, C.D. Holmes, D.J. Jacob, R. Yantosca, H. Skov, J.H. Christensen, S.A. Strode, R.B. Mason [2010] An Improved Global Model for Air-sea exchange of Mercury: High concentrations over the North Atlantic. *Environmental Science & Technology*, vol. 44 (22), pp. 8574-8580, doi: 10.1021/es102032g

Spokes L.J. and P.S. Liss [1995] Photochemically induced redox reactions in seawater, I. Cations. *Mar. Chem.*, vol. 49, pp. 201–213.

Stein E.D, Y. Cohen, A.M. Winer [1996] Environmental distribution and transformation of mercury compounds. Critical Review in *Environ. Sci. Technol.*, vol. 26, p 1.

Stoichev T., D. Amouroux, J. C. Wasserman, D. Point, A. D. Diego, G. Bareille, O. F. X. Donard [2004] Dynamics of mercury species in surface sediments of a macrotidal estuarine-coastal system (Ardour River, Bay of Biscay). *Estuarine, Coastal and Shelf Science*, vol. 59, pp. 511– 521.

Stordal M.C., G.A. Gill, L.-S. Wen, P.H. Santschi [1996] Mercury phase speciation in the surface waters of three Texas estuaries: Importance of colloidal forms. *Limnol. Oceanogr*., vol. 41, pp. 52–61.

Strode S., L. Jaeglé, S. Emerson [2010] Vertical transport of anthropogenic mercury in the ocean. *Glob. Biogeochem. Cycl.*, vol. 24, GB4014, doi:10.1029/2009GB003728.

Strode S.A., L. Jaegle´, N.E. Selin, D.J. Jacob, R.J. Park, R.M. Yantosca, R.P. Mason, F. Slemr [2007] Air-sea exchange in the global mercury cycle. *Global Biogeochem. Cy.* 2007, *21*, doi: 10.1029/2006GB002766.

Stumm W. [1992] Chemistry of the solid-water interface. *New York (NY): John Wiley&Sons, Inc*.

Sunderland E.M. and R.P. Mason [2007] Human impacts on open ocean mercury concentrations. *Global Biochemical Cycles*, vol. 21, GB4022, doi:10.1029/2006GB002876.

Sunderland E.M., F.A.P.C. Gobas, A. Heyes, B. Branfireun [2006] Environmental controls on the speciation and distribution of mercury in coastal sediments. *Marine Chemistry*, vol. 102, pp. 111-123.

Sunderland E.M., Gobas F.A.P.C., Heyes A., Branfireun B.A., Bayer A.K., Cranston R.E., Parsons M.B. [2004] Speciation and bioavailability of mercury in well-mixed estuarine sediments. *Mar. Chem*., vol. 90, pp. 91–105.

Travnikov, O., J.E. Jonson, A.S. Andersen, M. Gauss, A. Gusev, O. Rozovskaya, D. Simpson, V. Sokovyh, S.

Valiyaveetil and P. Wind, Development of the EMEP global modelling framework: progress report. Model Updates, EMEP/MSC-E Technical Report 7/2009, 2009

Tessier A. and D.R. Turner [1995] Metal speciation and bioavailability in aquatic systems. Wiley.

Ullrich S.M., T.W. Tanton, S.A. Abdrashitowa [2001] Mercury in the aquatic environment: a review of factors affecting methylation. Critical Reviews in *Environ. Sci. Technol*. vol. 31, p. 241.

Voelker B., F.M.M. Morel, B. Sulzberger [1997] Iron redox cycling in surface waters: effects of humic substances and light. *Environ. Sci. Technol*., vol. 31, pp. 1004–1011.

Vost E., M. Amyot, N. O'Driscoll [2012] Photoreactions of mercury in aquatic systems, in *Environmental Chemistry and Toxicology of Mercury*, First Edition, edited by G. Liu, Y. Cai, N. O'Driscoll, *John Wiley & Sons, Inc.*, pp.193-218.

Voughan P.P. and N.V. Blough [1998] Photochemical formation of hydroxyl radical by constituents of natural waters. *Environ. Sci. Technol*., vol. 32, pp. 2947–2953.

Weber J.H. [1993] Review of possible paths for abiotic methylation of mercury(II) in aquatic environment. *Chemosphere*, vol. 51, p. 2063.

Wen L.-S., P.H. Santschi, G.A. Gill, C. Paternostro [1999] Estuarine trace metal distribution in Galveston Bay: Importance of colloidal forms in the speciation of the dissolved phase. *Mar. Chem*., vol. 63, pp. 185–212.

Whalin L., and E.-H. Kim, R. Mason [2007] Factors influencing the oxidation, reduction, methylation and demethylation of mercury species in coastal waters. *Mar. Chem*., vol. 107, pp. 278–294.

Whalin L.M. and R.P. Mason [2006] A new method for the investigation of mercury redox chemistry in natural waters utilizing deflatable Teflon® bags and additions of isotopically labeled mercury. *Anal. Chim. Acta*, vol. 558, pp. 211–221.

Whalin L.M. [2005] The investigation of mercury redox chemistry in natural waters and the development of a new method for incubation experiments

Wild, O., A.M. Fiore, D.T. Shindell, R.M. Doherty, W.J. Collins, F.J. Dentener, M.G. Schultz, S. Gong, MacKenzie, G. Zeng, P. Hess, B. N. Duncan, D. J. Bergmann, S. Szopa, J.E. Jonson, . J. Keating, and A. Zuber: Modelling future changes in surface ozone: a parameterized approach. Atmos. Chem. Phys.., 12, 2037-2054, 2012.

Xiao Z.F., D. Stomberg, O. Lindqvist [1995] Influence of humic substances on photolysis of divalent mercury in aqueous solutions. *Water Air Soil Pollut.*, vol. 80, pp. 789–798.

Zafiriou O.C., M.B. True, E. Hayon [1987] Consequences of OH radical reaction in sea water: formation and decay of Br2 – ion radical. In: Zika, R.G., Cooper, W.J. (Eds.), Photochemistry of Environmental Aquatic Systems, ACS Symposium Series, *ACS*, pp. 89–105.

Zhang H. and S.E. Lindberg [2001] Sunlight and iron(III)-induced photochemical production of dissolved gaseous mercury in freshwater. *Environ. Sci. Technol.*, vol. 35, pp. 928–935.